OUKA
The University of Osaka
Institutional Knowledge Archive

Title	TsrA modulates type III secretion system 2 expression as a co-regulator of H-NS in Vibrio parahaemolyticus
Author(s)	Sutanto, Tan Paramita Wibowo
Citation	大阪大学, 2026, 博士論文
Version Type	VoR
URL	https://doi.org/10.18910/105604
rights	
Note	

The University of Osaka Institutional Knowledge Archive : OUKA

https://ir.library.osaka-u.ac.jp/

The University of Osaka

TsrA modulates type III secretion system 2 expression as a co-regulator of H-NS in *Vibrio parahaemolyticus*

DOCTORAL DISSERTATION

Submitted as partial fulfilment of the requirement to obtain Doctor of Philosophy Degree from Graduate School of Frontier Biosciences, The University of Osaka, Japan

March 2026

Tan Paramita Wibowo Sutanto

32A21705

Prof. Tetsuya Iida

Supervisor

ABSTRACT

TsrA modulates type III secretion system 2 expression as a co-regulator of H-NS in *Vibrio parahaemolyticus*

Tan Paramita Wibowo Sutanto

Vibrio parahaemolyticus is a gram-negative marine bacterium and a leading cause of seafood-borne gastroenteritis worldwide. The enteropathogenicity relies on type III secretion system 2 (T3SS2), encoded on a pathogenicity island and activated by a regulatory pathway centered on the transcriptional activator VtrB, which is antagonized by the xenogeneic silencer, histone-like nucleoid-structuring protein (H-NS). However, the complete transcriptional network is not yet fully understood. In this study, I identified TsrA as a negative regulator of T3SS2 gene expression. TsrA is a small protein conserved among *Vibrio* species that lacks a putative DNA-binding motif but has been implicated in the regulation of virulence genes in *V. cholerae*. In *V. parahaemolyticus*, deletion of *tsrA* increased VtrB production and T3SS2 secretion, thereby enhancing T3SS2-dependent pathogenicity. Transcription of *vtrB* occurs via a two-step activation process, in which TsrA affected the primary activation step, thereby modulating VtrB production. I further provide experimental evidence that TsrA physically interacts with H-NS via its C-terminal region, which correlates with its regulatory activity on *vtrB* expression. A systematic mutational analysis of the C-terminal 26 residues revealed several residues critical for TsrA regulatory activity. Moreover, the regulatory effect of TsrA on T3SS2 gene expression was dependent on H-NS, demonstrating that TsrA functions in concert with H-NS. Thus, my findings provide new insights into the regulatory mechanisms of virulence gene expression in *V. parahaemolyticus* by defining the role of TsrA in this network, while also placing TsrA among H-NS co-regulators.

TABLE OF CONTENTS

ABSTRACT 2

TABLE OF CONTENTS 3

LIST OF ABBREVIATIONS 5

LIST OF FIGURES 7

LIST OF TABLES 8

CHAPTER 1 9

GENERAL INTRODUCTION 9

1.1 A brief introduction to *Vibrio parahaemolyticus* 9

1.2 Pathogenicity and virulence of *Vibrio parahaemolyticus* 10

1.3 H-NS in the regulation of bacterial virulence genes 12

1.4 TsrA as a regulatory factor in *Vibrio* species 15

CHAPTER 2 18

METHODOLOGY 18

2.1 Ethics Statement 18

2.2 Bacterial strains, primers, plasmids, and growth conditions 18

2.3 Protein sample preparation and analysis 18

2.4 Cell culture and cytotoxicity assay 20

2.5 Rabbit ileal loop assay 20

2.6 RNA sequencing 21

2.7 Northern blot analysis and qRT-PCR 21

2.8 Purification of TsrA-interacting protein 22

2.9 Direct interaction between TsrA and H-NS 23

2.10 Co-immunoprecipitation 24

2.11 Structural modeling 25

2.12 Data availability 25

CHAPTER 3 36

RESULTS 36

3.1 TsrA negatively affects T3SS2 gene expression 36

3.2 TsrA affects primary activation of *vtrB* gene expression 38

3.3 TsrA negatively affects T3SS2-dependent virulence 40

3.4 TsrA interacts with H-NS 41

CHAPTER 4 47

DISCUSSION 47

CHAPTER 5 51

CONCLUDING REMARKS 51

REFERENCES 52

ACKNOLEDGEMENTS 58

AUTHOR'S ACHIEVEMENT 60

LIST OF ABBREVIATIONS

anti-DIG-AP: anti-digoxigenin-alkaline phosphatase

BSA: bovine serum albumin

CBB: coomassie brilliant blue

CFU: colony forming unit

Ctrl: Control

DMEM: Dulbecco's modified Eagle's medium

DNA: deoxyribonucleic acid

FA: fluid accumulation

H-NS: histone-like nucleoid-structuring protein

HRP: horseradish peroxidase

KP: Kanagawa phenomenon

LB: Luria-Bertani

LC-MS/MS: Liquid Chromatography-Tandem Mass Spectrometry

LDH: lactase dehydrogenase

MOI: multiplicity of infection

NAPs: nucleoid-associated proteins

Ni-NTA: Nickel-Nitrilotriacetic Acid

OMP: outer membrane protein

PAE: predicted aligned error

PCR: polymerase chain reaction

pLDDT: predicted Local Distance Difference Test

PVDF: polyvinylidene difluoride

RNA: ribonucleid acid

RNAP: RNA polymerase

SD: standard deviation

SDS: sodium dodecyl sulfate

SDS-PAGE: sodium dodecyl sulfate-polyacrylamide gel electrophoresis

T3SS: type III secretion system

T6SS: type VI secretion system

TCA: trichloroacetic acid

TDH: thermostable direct hemolysin

TsrA: type VI secretion system regulator A

Vp-PAI: *V. parahaemolyticus* pathogenicity island

WT: wild type

qRT-PCR: quantitative real time polymerase chain reaction

LIST OF FIGURES

Figure	**Page**
1. *Vibrio parahaemolyticus* cell morphology.	9
2. The sequencing result of the genome of *V. parahaemolyticus* strain RIMD2210633 contains two circular chrosomes.	10
3. Structure of Type III Secretion System (T3SS).	11
4. Regulation of T3SS2 gene expression during the non-permissive and permissive condition.	12
5. Filament-based mechanism of H-NS gene silencing.	13
6. Schematic representation of an H-NS dimer bound to two molecules of Hha.	15
7. Schematic representation of the domain organization of TsrA and H-NS.	16
8. TsrA negatively affects the expression of T3SS2 genes.	37
9. VtrA reduction in Δ*tsrA* is mediated by VtrB.	38
10. TsrA affects the initial activation of *vtrB* transcription.	39
11. TsrA negatively affects the T3SS2-dependent virulence.	41
12. TsrA interacts with H-NS.	43
13. TsrA directly interacts with H-NS (comparison with BSA as negative control).	44
14. Mutational analysis of the C-terminal region of TsrA.	45
15. Structural modeling of the TsrA-H-NS complex predicted by AlphaFold3.	46
16. The regulatory activity of TsrA is dependent on H-NS.	50

LIST OF TABLES

Table	**Page**
1. *V. parahaemolyticus* strains used in this study.	26
2. *E. coli* strains used in this study.	26
3. Plasmids used in this study.	27
4. Primers used in this study.	29

CHAPTER 1

GENERAL INTRODUCTION

1.1 A brief introduction to *Vibrio parahaemolyticus*

Vibrio parahaemolyticus is a rod-shaped gram-negative, facultative anaerobic marine bacterium measuring 1–3 μm in length (Figure 1). In 1950, an outbreak of acute gastroenteritis linked to the consumption of dried sardines ("shirasu" in Japanese) occurred in Osaka, Japan, affecting 272 individuals and resulting in 20 deaths. This bacterium was isolated as a causative agent of this outbreak by Dr. Tsunesaburo Fujino, a professor at Research Institute for Microbial Diseases (1). Since then, *V. parahaemolyticus* has been recognized as a major seafood-borne pathogen worldwide (2, 3). This halophilic bacterium inhabits marine and estuarine environments around the world, and thereby the infections occur through the consumption of raw or undercooked seafood contaminated with the bacterium (2, 4, 5). The incubation period is short, usually ranging from several hours to 24 hours, and symptoms typically manifest as acute gastroenteritis characterized by diarrhea, abdominal pain, nausea, and vomiting.

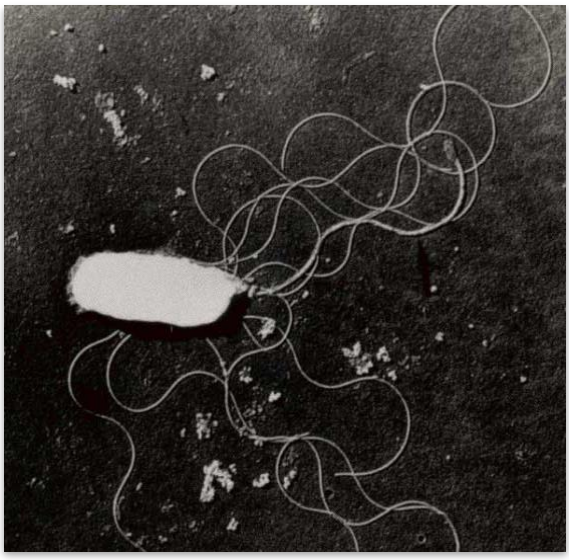


Figure 1. *Vibrio parahaemolyticus* cell morphology.

1.2 Pathogenicity and virulence of *Vibrio parahaemolyticus*

In 2003, the whole genome of a clinical isolate of *V. parahaemolyticus*, strain RIMD2210633, was first sequenced through shotgun sequencing (6). The genome consists of two circular chromosomes (Figure 2). The genome sequencing revealed the presence of two sets of type III secretion systems (T3SSs) (6): type III secretion system 1 (T3SS1), encoded on the larger chromosome and type III secretion system 2 (T3SS2), encoded on the smaller chromosome.

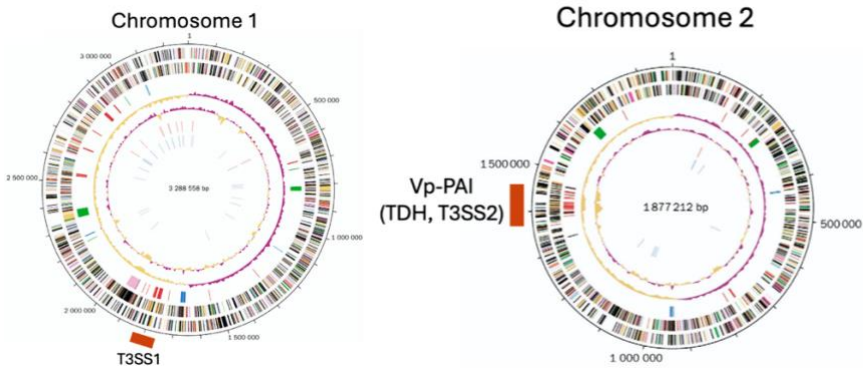


Figure 2. The sequencing result of the genome of *V. parahaemolyticus* strain RIMD2210633 contains two circular chrosomes. T3SS1 and T3SS2 revealed in each chromosome following TDH at chromosome 2 (indicated by orange lines).

T3SS is a syringe-like specialized protein secretion system that directly injects bacterial proteins, called effectors, into the eukaryotic host cytoplasm and contributes to bacterial virulence (7). This apparatus consists of three main components that are essential for its functions such as basal body, needle, and translocon (Figure 3). Further studies have displayed that T3SS1 contributes to cytotoxicity, while T3SS2 plays a major role in enterotoxicity, establishing T3SS2 as a key virulence determinant of *Vibrio parahaemolyticus* (3, 8).

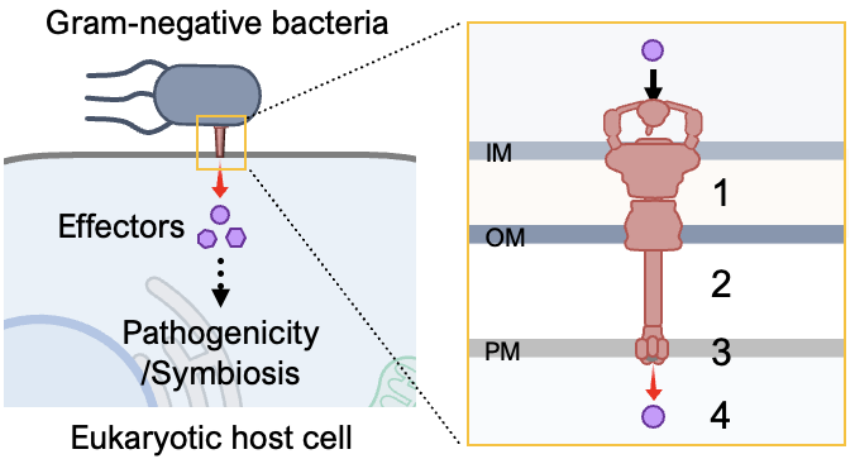


Figure 3. Structure of Type III Secretion System (T3SS). T3SS components including basal body (1), needle (2), translocon (3), and effector (4).

The expression of T3SS2-related genes are encoded on the 80-kb *V. parahaemolyticus* pathogenicity island (Vp-PAI), whose expression is regulated by two transcriptional regulators, VtrA and VtrB (9, 10). VtrA and VtrB are both transmembrane proteins encoded in Vp-PAI. VtrA activates the gene expression of VtrB, which in turn activates the Vp-PAI gene expression. VtrA forms a complex with its co-transcribed protein, VtrC (11). The VtrA/VtrC complex binds near the -35 element of the *vtrB* promoter to initiate *vtrB* transcription. This activation requires ToxR, which binds upstream of the VtrA-binding site in the *vtrB* promoter (12). Following this initial activation, VtrB amplifies its own expression through a positive feedback loop, in which the transcription of the VtrB-regulated operon located upstream of *vtrB* extends across the terminator into the *vtrB* gene in a read-through manner. This autoregulatory loop further enhances T3SS2 gene expression and is critical for the pathogenicity of *V. parahaemolyticus* (12). Conversely, *vtrB* gene expression is repressed by the global transcriptional repressor H-NS (13). It is affected by external environmental conditions such as temperature and salinity. The expression is induced at 37°C and 0.1 M NaCl (the permissive condition), while it is not expressed at lower temperature or higher salinity (the non-permissive

conditions) (13). H-NS binds upstream of the *vtrB* gene, where it antagonizes the binding of VtrA and ToxR to the *vtrB* promoter. Thus, this complex regulatory network coordinates the fine-tuned expression of T3SS2 genes in *V. parahaemolyticus* (Figure 4).

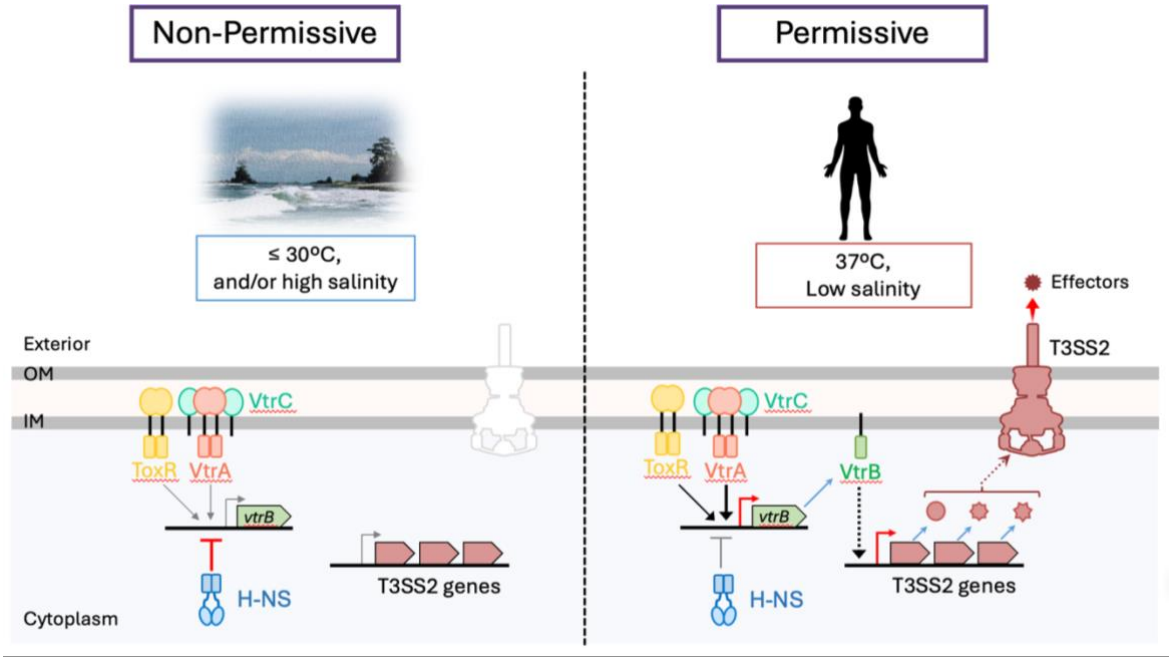


Figure 4. Regulation of T3SS2 gene expression during the non-permissive and permissive condition (13).

1.3 H-NS in the regulation of bacterial virulence genes

Pathogenic bacteria rely on complex regulatory networks to precisely control the expression of virulence genes in response to environmental and host-associated cues (14). In Gram-negative bacteria, repression of horizontally acquired loci is frequently mediated by nucleoid-associated proteins, among which H-NS has been most extensively characterized. These repressed genes are often located within horizontally acquired DNA regions, such as pathogenicity islands and other mobile genetic elements (15).

Through this activity, H-NS serves a critical function in xenogeneic silencing, thereby limiting the potentially deleterious expression of foreign genes while allowing for their

regulated deployment during infection (16, 17). At the molecular level, H-NS represses transcription through filament-based mechanisms that depend on its ability to oligomerize along DNA (Figure 5). H-NS-mediated silencing can occur by limiting the access of RNA polymerase to promoter regions, thereby inhibiting transcription initiation, or by interfering with transcription elongation after initiation has occurred (18, 19). These effects are mediated by the formation of extended H-NS nucleoprotein filaments that assemble along regulatory DNA regions, including promoters and downstream coding sequences (19).

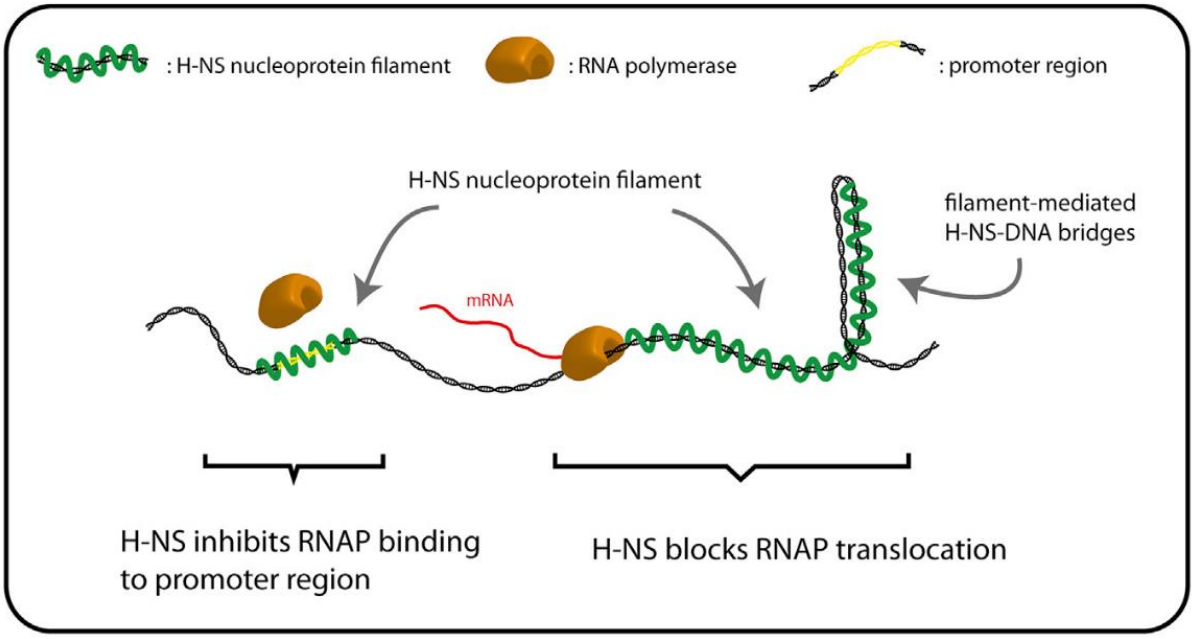


Figure 5. Filament-based mechanism of H-NS gene silencing (19).

In addition to filament formation, H-NS can bridge separate DNA segments, generating higher-order nucleoprotein structures that constrain DNA flexibility and further restrict the accessibility of regulatory regions to the transcriptional machinery (18, 19). Such DNA architectural changes provide multiple physical mechanisms by which H-NS effectively suppresses gene expression, particularly for genes located within horizontally acquired genomic regions (17).

Importantly, the repressive activity of H-NS is not static but is influenced by environmental conditions. Prior research revealed that temperature influences the stability of H-NS-DNA complexes, with elevated, host-associated temperatures reducing the stability of H-NS filaments and alleviating transcriptional repression, whereas lower temperatures favor stronger DNA binding and enhanced silencing (16, 19). This thermoresponsive behavior allows H-NS to contribute to environmentally regulated gene expression, including the activation of virulence-associated genes under host-relevant conditions (16).

Furthermore, H-NS function can be adjusted through interactions with accessory regulatory proteins that modify its oligomerization properties, DNA-binding behavior, or higher-order complex formation (20). Such modulation enables bacteria to maintain foreign genes in a repressed state under non-permissive conditions while permitting their rapid activation when beneficial, underscoring the importance of H-NS-associated factors in the regulation of horizontally acquired virulence genes.

H-NS is understood to operate in conjunction with accessory regulatory proteins that modulate its repressive activity, thereby fine-tuning the expression of horizontally acquired genes. Well-characterized examples include the H-NS paralog StpA in *Escherichia coli* and the H-NS-associated protein Hha in *Salmonella*. While StpA retains DNA-binding activity and can directly associate with target DNA (21), Hha lacks intrinsic DNA-binding capacity and instead regulates gene expression through protein-protein interactions with H-NS (Figure 6), a process that may involve conformational changes that influence H-NS function (22). However, no H-NS co-regulator has previously been reported in *Vibrio* species.

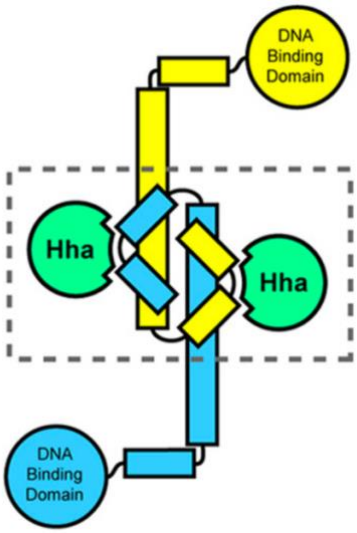


Figure 6. Schematic representation of an H-NS dimer bound to two molecules of Hha (22).

1.4 TsrA as a regulatory factor in *Vibrio* species

TsrA (type VI secretion system regulator A) is a small protein of approximately 94 amino acids that is conserved among *Vibrio* species (23). It was initially characterized in *Vibrio cholerae* as a negative regulator of virulence-associated gene expression (24). Studies in *V. cholerae* discovered that TsrA represses the expression of multiple virulence determinants, including cholera toxin, the toxin-coregulated pilus, and genes associated with the type VI secretion system in *V. cholerae* (23–26). A genome-wide analysis revealed that a substantial proportion of TsrA-regulated genes are located within horizontally acquired genomic islands. This observation suggests that TsrA may contribute to the silencing of foreign DNA, a function that parallels the established role of H-NS in xenogeneic silencing (25). The enrichment of TsrA targets within AT-rich regions further supports the notion that TsrA influences the expression of genes that are subject to H-NS-mediated repression. In addition, TsrA exhibits structural homology to the oligomerization domain of H-NS (25), suggesting that these proteins may share common modes of protein–protein interaction. However, unlike H-NS, TsrA lacks a recognizable DNA-binding domain (Figure 7). This structural distinction suggests that TsrA

does not directly interact with DNA but instead regulates gene expression indirectly, potentially through interactions with other DNA-binding regulatory proteins (23).

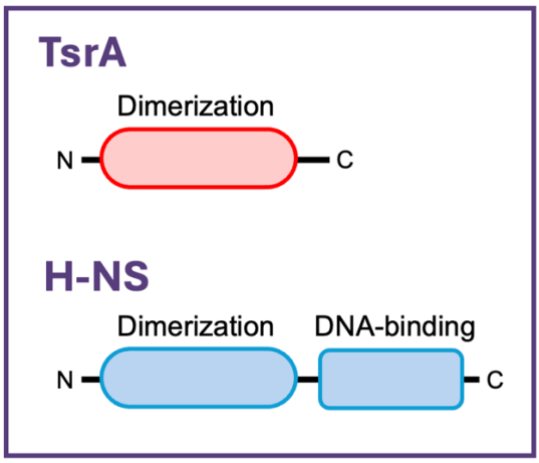


Figure 7. Schematic representation of the domain organization of TsrA and H-NS.

A recent study examining the combined effects of TsrA and H-NS deletion have further supported their functional relationship (23). While H-NS and TsrA were found to synergistically regulate a subset of genes, loss of H-NS accounted for the majority of transcriptional changes observed in an *hns tsrA* double mutant. In contrast, deletion of *tsrA* alone resulted in comparatively modest changes in gene expression. These findings indicate that TsrA does not function as a dominant global regulator but instead exerts its effects primarily through modulation of H-NS activity or through interaction with other regulatory factors that act on DNA. Notably, TsrA is phylogenetically restricted to members of the order *Vibrionales* and the related species *Plesiomonas shigelloides* (25), suggesting that it represents a lineage-specific adaptation that fine-tunes gene regulation in these organisms.

In *V. parahaemolyticus*, expression of T3SS2 genes is tightly regulated and evidence suggested that it is strongly influenced by H-NS, which represses T3SS2 transcription under non-inducing conditions. Relief of H-NS-mediated repression is therefore a critical step in the activation of T3SS2 during infection. Although the functional and structural relationship

between H-NS and TsrA was implicated in *V. choleare*, the role of TsrA in *V. parahaemoltyicus*, and more broadly in non-*cholerae Vibrio* species, has not been previously explored. Addressing this knowledge gap is essential for understanding how *V. parahaemolyticus* integrates global and accessory regulatory mechanisms to control virulence gene expression.

In this study, I investigate the role of TsrA in the regulation of T3SS2 gene expression and assess its contribution to the pathogenicity of *Vibrio parahaemolyticus*, providing new insights into the regulatory strategies that shape virulence in *V. parahaemolyticus*.

CHAPTER 2

METHODOLOGY

2.1 Ethics Statement

All animal experiments in this study were approved by the Animal Care and Use Committee of the Research Institute for Microbial Diseases, The University of Osaka, and were performed in strict accordance with the institute's guidelines for the Care and Use of Laboratory Animals.

2.2 Bacterial strains, primers, plasmids, and growth conditions

The clinical isolate *Vibrio parahaemolyticus* RIMD2210633 (6) was used as the wild-type strain. *E. coli* DH5α and BW19851 were used for DNA manipulation. All bacterial strains and plasmids used in this study are listed in Tables 1 to Table 3. The primers used are listed in Table 4. Deletion mutants were generated using a four-primer PCR strategy following a previously reported method (27). Plasmids encoding TsrA–6×His derivatives, in which residues 69–94 in the C-terminal region were individually substituted with alanine or serine if the original residue was alanine, were constructed by site-directed mutagenesis using the appropriate primer pairs. *V. parahaemolyticus* strains were grown at 37˚C in Luria–Bertani (LB) medium (Lennox: tryptone, 1%; yeast extract, 0.5%; NaCl, 0.5%). Appropriate antibiotics were added to grow the plasmid-carrying strains: 50 μg/ml kanamycin for pET28a and pE-SUMO-Kan, and 15 μg/ml chloramphenicol for pSA19CP plasmid backgrounds.

2.3 Protein sample preparation and analysis

V. parahaemolyticus strains were grown in LB medium at 37°C to an optical density at 600 nm (OD_{600}) of 1.8. The culture was centrifuged at 15,000 × *g* for 5 min to separate the

pellets containing the bacterial cells from the supernatants containing the secreted proteins. Cell pellets were resuspended in SDS-PAGE sample buffer, sonicated, and heat-denatured at 95°C for 5 min, and used as whole-cell lysates. Secreted proteins were precipitated from the supernatants with ice-cold 10% (v/v) trichloroacetic acid (TCA) on ice for 2 h, followed by centrifugation at 25,000 × *g* for 30 min. The resulting pellets were rinsed with cold acetone, solubilized in SDS-PAGE sample buffer, and denatured at 95°C for 5 min. Proteins were then separated by SDS-PAGE and either visualized by CBB staining or transferred to polyvinylidene difluoride (PVDF) membranes for immunoblotting. The membranes were probed with primary antibodies against the proteins of interest. Anti-VtrA, anti-VtrB, and anti-VopD2 polyclonal antibodies were described elsewhere (9, 27). Monoclonal antibodies against anti-His-tag (clone OGHis, Medical & Biological Laboratories) and anti-FLAG (clone M2, Sigma-Aldrich) were purchased from commercial suppliers. The membranes were then probed with horseradish peroxidase (HRP)-conjugated goat anti-rabbit antibodies (code: 62-1820, Invitrogen) or HRP-conjugated rabbit anti-mouse antibodies (code: 61-6520, Invitrogen). The blots were developed using the ECL Prime Western Blotting Detection Reagent (GE Healthcare). Whole-cell lysate proteins with CBB staining of each sample were used as loading controls for immunoblotting. To detect TsrA–6×His and its derivatives, whole-cell lysates were futher concentrated by TCA precipitation, or the proteins were enriched from *V. parahaemolyticus* lysates using Ni-NTA pull-down as follows. *V. parahaemolyticus* strains were grown in LB medium at 37°C to OD_{600} of 1.8. Bacterial cells were harvested by centrifugation at 15,000 × *g* for 5 min and lysed by sonication (10 s pulse, 30 s interval on ice, 10 cycles), repeated seven times, in Ni-NTA running buffer (25 mM Tris-HCl, 50 mM NaCl, pH 8.0) containing a protease inhibitor cocktail (P8849, Sigma-Aldrich), 40 U/mL benzonase (Sigma-Aldrich), and 1 mg/mL lysozyme (Sigma-Aldrich). The lysate was incubated with Ni-NTA His·Bind beads (Novagen) on a rotary shaker for 2 h at 4°C, to capture His-tagged

proteins. The beads were washed five times with Ni-NTA wash buffer (25 mM Tris-HCl, 50 mM NaCl, 60 mM imidazole, pH 8.0), and bound proteins were eluted with Ni-NTA elution buffer (25 mM Tris-HCl, 200 mM NaCl, 500 mM imidazole, pH 8.0). The eluates were analyzed by immunoblotting using anti-His-tag antibody.

2.4 Cell culture and cytotoxicity assay

Caco-2 cells (ECACC 86010202) supplied by the European Collection of Authenticated Cell Cultures were maintained in Dulbecco's modified Eagle's medium (DMEM) supplemented with 10% fetal bovine serum and 100 μg/ml gentamicin at 37°C under 5% CO_2. Cytotoxicity assays were performed as previously described (28), with minor modifications. Briefly, 2×10^4 Caco-2 cells were seeded into each well of a 96-well plate and incubated for 48 h. The cells were washed twice with phosphate-buffered saline, and the medium was replaced with fresh phenol red-free DMEM. The cells were then infected with each *V. parahaemolyticus* strain at a multiplicity of infection (MOI) of 10. Cytotoxicity was assessed by measuring the release of lactate dehydrogenase (LDH) into the culture supernatants using a Cytotoxicity LDH Assay Kit-WST (Dojindo) according to the manufacturer's instructions. The percentage of cytotoxicity was calculated as follows: [OD_{490} of experimental release–OD_{490} of spontaneous release] / [OD_{490} of maximum release–OD_{490} of spontaneous release] × 100. Spontaneous release refers to the amount of LDH released from uninfected cells, whereas maximum release refers to the total LDH released after complete lysis of uninfected cells by detergent.

2.5 Rabbit ileal loop assay

Rabbit ileal loop tests were performed as previously described (28). Briefly, *V. parahaemolyticus* strains were grown in LB medium. The cells were harvested by

centrifugation and suspended in LB medium. One milliliter of the bacterial suspension (10^9 colony-forming units) was injected into the ligated ileal loops of a 1.5–2-kg female New Zealand White rabbit (loop length ~8 cm). Fluid accumulation in each loop was measured 16 h after inoculation. The fluid accumulation (FA) ratio was calculated as the volume of accumulated fluid (mL) per length of the ligated rabbit small intestine (cm).

2.6 RNA sequencing

Total RNA was extracted from *V. parahaemolyticus* as described previously (13). Briefly, *V. parahaemolyticus* cells were grown in LB containing 0.5% NaCl at 37°C to an OD_{600} of ~1. RNAprotect Bacterial Reagent (Qiagen) was added to the culture to stabilize RNA, and total RNA was extracted using the RNeasy Mini Kit (Qiagen) with DNase I treatment, according to the manufacturer's instructions. Purified RNA samples were analyzed using PCR to confirm the absence of DNA contamination. The concentration of each sample was measured using a NanoDrop ND-1000 spectrophotometer (Thermo Fisher).

RNA libraries were prepared using the TruSeq Stranded Total RNA with RiboZero Plus Kit (Illumina). Whole-transcriptome sequencing was carried out on an Illumina NovaSeq 6000 platform in the 151-bp single-end mode. Sequence reads were mapped to the *V. parahaemolyticus* reference genome (GCF_000196095.1) using Bowtie2 v2.4.4 (29), and the gene counts were obtained using HTSeq v0.11.1 (30). The read counts data were uploaded onto iDEP 2.20.4 (31) and differential gene expression was analyzed using the DESeq2 option.

2.7 Northern blot analysis and qRT-PCR

V. parahaemolyticus strains were grown in LB medium to an OD_{600} of 0.8 at 25˚C, a non-permissive condition for *vtrB* expression, and then shifted to 37˚C to induce *vtrB* transcription. RNA was extracted at 0, 15, 30, and 60 min after induction using the hot-acidic phenol method

(32). Northern blotting was performed as previously described (12). Briefly, total RNA (2.5 μg) was heated at 60°C and separated by electrophoresis on a 1.2% agarose gel containing formaldehyde alongside Dyna Marker (Prestain Marker for RNA High; BioDynamics Laboratory Inc). The RNA was then transferred overnight onto a positively charged nylon membrane (Roche) using 20×SSC buffer (3 M NaCl, 0.3 M sodium citrate dehydrate) and cross-linked by UV irradiation (1200×100 μJ/cm²). Hybridization was carried out at 50°C for 4 h in DIG Easy Hyb buffer (Roche) using the DIG-labeled P_{vtrB} probe (12). After hybridization, the membrane was washed with a high-stringency buffer (0.1×SSC, 0.1% SDS), blocked for 30 min in blocking solution (Roche), and incubated for 1 h with anti-digoxigenin-alkaline phosphatase (anti-DIG-AP; Roche). The blots were developed using CDP-STAR chemiluminescent substrate (Roche) and visualized using an Amersham ImageQuant 800 system (Cytiva). Ribosomal RNA was stained with GelRed (Biotium, Hayward, CA, USA) and visualized by UV irradiation as the loading control. qRT-PCR was performed as previously described (12) using SYBR Green RNA-direct Real-time PCR Master Mix (Toyobo) on a QuantStudio 5 real-time PCR system (Thermo Fisher). Relative mRNA transcript levels were calculated using the threshold cycle ($2^{-\Delta\Delta CT}$) method and normalized to the housekeeping gene *recA*.

2.8 Purification of TsrA-interacting proteins

Protein expression was performed as previously described (13). Briefly, the gene for C-terminally 6×His-tagged TsrA (TsrA-6×His) or its derivative was inserted into the pET28a expression plasmid (Novagen), yielding TsrA-6×His constructs. *E. coli* BL21 (DE3) cells carrying these plasmids were grown in LB medium with 50 μg/ml kanamycin at 37°C to an OD_{600} of ~0.6. Protein expression was induced by adding 1 mM isopropyl-1-thio-β-D-galactopyranoside, followed by further incubation at 37°C for 4 h. Bacterial cells were

harvested by centrifugation at 10,000 × *g* for 15 min and lysed in CelLytic B cell lysis reagent (Sigma-Aldrich) containing a protease inhibitor cocktail (P8849, Sigma-Aldrich), 40 U/mL benzonase (Sigma-Aldrich), and 1 mg/mL lysozyme (Sigma-Aldrich), followed by sonication (10 s pulse, 30 s interval on ice, 10 cycles), repeated seven times. The cell lysates were centrifuged at 10,000 × *g* for 15 min, and the resulting supernatants, including solubilized proteins, were filtered through a 0.22-μm filter to remove insolubilized proteins and unbroken cells. Each 6×His-tagged protein was immobilized on Ni-NTA His·Bind beads (Novagen) packed in a column, according to the manufacturer's protocol. For purification of TsrA-interacting proteins, *V. parahaemolyticus* Δ*tsrA* strain grown in LB medium was lysed in Ni-NTA running buffer (25 mM Tris-HCl, 50 mM NaCl, pH8.0) containing a protease inhibitor cocktail (P8849, Sigma-Aldrich), 40 U/mL benzonase (Sigma-Aldrich), and 1 mg/mL lysozyme (Sigma-Aldrich), and the lysate was incubated with TsrA-6×His-immobilized beads on a rotary shaker for 2 h at 4°C. The beads were washed five times with Ni-NTA wash buffer (25 mM Tris-HCl, 50 mM NaCl, 60 mM imidazole, pH 8.0), and bound proteins were eluted from the beads with Ni-NTA elution buffer (25 mM Tris-HCl, 200 mM NaCl, 500 mM imidazole, pH 8.0). The eluates were subjected to SDS–PAGE followed by CBB staining or LC-MS/MS analysis with a timsTOF Pro (Bruker) at Core Instrumentation Facility, Research Institute for Microbial Diseases, The University of Osaka, as described previously (13). Proteins were identified by searching the database using Mascot (Matrix Science).

2.9 Direct interaction between TsrA and H-NS

For purification of C-terminally 3×FLAG-tagged H-NS (H-NS-3×FLAG), the gene encoding H-NS-3×FLAG was inserted into pE-SUMO-Kan (LifeSensors) to generate the 6×His-SUMO-tagged H-NS-3×FLAG. The C-terminal region of *ULP1* encoding SUMO protease (403–621 aa, Ulp1C) was cloned into pET28a to yield 6×His-U1p1C. *E. coli* BL21

(DE3) or Rosetta-gami 2 (DE3) (Novagen) cells harboring the respective plasmids were grown in LB medium with 50 μg/ml kanamycin to an OD_{600} of 0.6. Protein expression was induced by adding 0.1 mM isopropyl-1-thio-β-D-galactopyranoside (Sigma), followed by incubation for 4 h at 37°C for 6×His-SUMO-tagged H-NS-3×FLAG or for 16 h at 20°C for 6×His-Ulp1C. Expressed 6×His-SUMO-tagged H-NS-3×FLAG and 6×His-Ulp1C were purified using Ni-NTA His·Bind beads (Novagen) according to the manufacturer instructions. The 6×His-SUMO-tag was cleaved from the purified 6×His-SUMO-tagged H-NS-3×FLAG by 6×His-tagged Ulp1C in a digestion buffer (20 mM Tris-HCl, 150 mM NaCl, 1 mM dithiothreitol, pH 7.6) at 30°C for 24 h, and then passed through TALON Metal Affinity Resin (Takara) columns to remove the released His-SUMO tag, undigested fusion proteins, and 6×His-Ulp1C, yielding the H-NS-3×FLAG protein. The purity of the purified protein was confirmed by SDS–PAGE followed by CBB staining. Protein concentrations were measured using a Nanodrop ND-1000. To examine the direct interaction between TsrA and H-NS, Ni-NTA His·Bind beads immobilized with TsrA-6×His or control bead was incubated with 25 μM purified H-NS-3×FLAG protein or bovine serum albumin (BSA) on a rotary shaker for 2 h at 4°C. The beads were washed five times with the washing buffer and then eluted with the elution buffer. The eluates were subjected to SDS–PAGE, followed by CBB staining or immunoblotting with anti-His and anti-FLAG antibodies.

2.10 Co-immunoprecipitation

To construct a *V. parahaemolyticus* strain expressing TsrA-6×His and H-NS-3×FLAG, the *tsrA* gene was deleted from the HNS-3F strain, which chromosomally expresses H-NS-3×FLAG (13), resulting in the HNS-3FΔ*tsrA* strain. The plasmid pSA19CP encoding *tsrA*-6×His (pTsrA-6×His), its derivatives, or the empty vector was introduced into this strain, yielding strains expressing TsrA-6×His, its derivatives, or harboring the empty vector as a

control strain. These strains, along with the Δ*tsrA* strain harboring pTsrA-6×His, were grown in LB medium and lysed in Ni-NTA running buffer (25 mM Tris-HCl, 50 mM NaCl, pH 8.0) containing a protease inhibitor cocktail (P8849, Sigma-Aldrich), 40 U/mL benzonase (Sigma-Aldrich), and 1 mg/mL lysozyme (Sigma-Aldrich). The lysates were subjected to co-immunoprecipitation using anti-FLAG M2 beads (Sigma-Aldrich). The beads were washed five times with FLAG washing buffer (20 mM Tris-HCl, 200 mM KCl, 5 mM $MgCl_2$, 10% glycerol, pH 8.0), and eluted using 2×SDS-PAGE sample buffer. The eluates were analyzed by immunoblotting with anti-His and anti-FLAG antibodies.

2.11 Structural modeling

Models of the H-NS and TsrA complexes were generated using AlphaFold3 (https://alphafoldserver.com) (33) with *Vibrio parahaemolyticus* TsrA (uniprot: Q87KF9) and H-NS (uniprot: Q87QL6) protein sequences as inputs. The resulting structural models were visualized using ChimeraX (34).

2.12 Data availability

The RNA-seq datasets in this study were deposited in the NCBI Sequence Read Archive (SRA) under the accession number PRJNA1357053.

Table 1. *V. parahaemolyticus* strains used in this study

Strains	Genotypes/descriptions	References
RIMD2210633 (WT)	Clinical isolate, serotype O3:K6, *tdh*$^+$ and T3SS2$^+$	Laboratory collection
Δ*tsrA*	RIMD2210633 *tsrA* (*vp3018*)	This study
Δ*vtrB*	RIMD2210633 *vtrB* (*vpa1348*)	(9)
Δ*vtrB* Δ*tsrA*	RIMD2210633 *vtrB tsrA*	This study
Δ*hns*	RIMD2210633 *hns* (*vp1133*)	(13)
Δ*hns* Δ*tsrA*	RIMD2210633 *hns tsrA*	This study
HNS-3F	RIMD2210633 *hns*::*hns-3xFLAG*	(13)
POR-2	RIMD2210633 *tdhA tdhS vcrD1* (T3SS1$^-$)	(27)
POR-2 Δ*tsrA*	POR-2 *tsrA*	This study
ΔT3SS2	POR-2 *vcrD2*	(35)

Table 2. *E. coli* strains used in this study

Strains	Genotypes/descriptions	References
DH5α	F$^-$ Φ80Δ*lacZ*M15 Δ(*lacZYA argF*)U169 *deoP recA1 endA1 hsdR17*(rK$^-$ mK$^-$)	Laboratory collection
BW19851	F$^-$ *RP4-2*(*Km::Tn7,Tc::Mu-1*) Δ*uidA3::pir+ recA1 endA1 thiE1 hsdR17 creC510*	Laboratory collection
BL21(DE3)	F$^-$ *omp*T, *hsdSB* (*r*B$^-$, *m*B$^-$), *dcm*, *gal*, λ(DE3)	Laboratory collection

Table 3. Plasmids used in this study

Plasmids	Description	References
pYAK1	oriR6K-based suicide vector for gene replacement, Cm^R	(36)
pYAK-Δ*tsrA*	A derivative of pYAK1 for deletion of *tsrA* gene	This study
pSA19CP	Complementation vector for *V. parahaemolyticus*, Cm^R	(37)
p*tsrA*	pSA19CP containing *tsrA* gene with its 300 bp upstream region	This study
p*tsrA*-6H	p*tsrA* derivative carrying *tsrA* with a C-terminal 6×His tag	This study
p*tsrA*Δ*C*-6H	p*tsrA*-6H derivative expressing C-terminally truncated *tsrA* (1–68)-6×His	This study
p*tsrA*-Q69A-6H	p*tsrA*-6H with Q69A mutation	This study
p*tsrA*-V70A-6H	p*tsrA*-6H with V70A mutation	This study
p*tsrA*-E71A-6H	p*tsrA*-6H with E71A mutation	This study
p*tsrA*-L72A-6H	p*tsrA*-6H with L72A mutation	This study
p*tsrA*-L73A-6H	p*tsrA*-6H with L73A mutation	This study
p*tsrA*-A74S-6H	p*tsrA*-6H with A74S mutation	This study
p*tsrA*-K75A-6H	p*tsrA*-6H with K75A mutation	This study
p*tsrA*-D76A-6H	p*tsrA*-6H with D76A mutation	This study
p*tsrA*-L77A-6H	p*tsrA*-6H with L77A mutation	This study
p*tsrA*-A78S-6H	p*tsrA*-6H with A78S mutation	This study
p*tsrA*-Q79A-6H	p*tsrA*-6H with Q79A mutation	This study
p*tsrA*-Q80A-6H	p*tsrA*-6H with Q80A mutation	This study
p*tsrA*-G81A-6H	p*tsrA*-6H with G81A mutation	This study

Plasmids	Description	References
p*tsrA*-I82A-6H	p*tsrA*-6H with I82A mutation	This study
p*tsrA*-S83A-6H	p*tsrA*-6H with S83A mutation	This study
p*tsrA*-A84S-6H	p*tsrA*-6H with A84S mutation	This study
p*tsrA*-D85A-6H	p*tsrA*-6H with D85A mutation	This study
p*tsrA*-E86A-6H	p*tsrA*-6H with E86A mutation	This study
p*tsrA*-L87A-6H	p*tsrA*-6H with L87A mutation	This study
p*tsrA*-L88A-6H	p*tsrA*-6H with L88A mutation	This study
p*tsrA*-A89S-6H	p*tsrA*-6H with A89S mutation	This study
p*tsrA*-Y90A-6H	p*tsrA*-6H with Y90A mutation	This study
p*tsrA*-L91A-6H	p*tsrA*-6H with L91A mutation	This study
p*tsrA*-N92A-6H	p*tsrA*-6H with N92A mutation	This study
p*tsrA*-K93A-6H	p*tsrA*-6H with K93A mutation	This study
p*tsrA*-Q94A-6H	p*tsrA*-6H with Q94A mutation	This study
p*hns*-3F	pSA19CP containing *hns* gene with its 500 bp upstream region and a C-terminal 3 ×FLAG tag	(13)
pET28a	Expression vector for *E. coli*, Km^R	Novagen
pET28a-*tsrA*-6H	pET28a containing *tsrA* with a C-terminal 6×His tag, for expression TsrA-6×His	This study
pET28a-*tsrA*ΔC-6H	pET28a-*tsrA*-6H derivative expressing C-terminally truncated *tsrA* (1–68)-6×His	This study
pE-SUMO-*hns*-3F	pE-SUMO-Kan containing *hns-3×FLAG*	This study

Table 4. Primers used in this study

Primers	**Sequence (5' to 3')**	**Description**
vtrB-promoter-F	CGCTGAGCCCTTTTCACAG	For Northern blotting and qRT-PCR
vtrB-promoter-R	GGAGTTTGAAGTGGTCGTC	
dVP3018/*tsrA*-1	GGGGATCCTTGGCACCGAAGTTCATG GAACG	For construction of pYAK-Δ*tsrA*
dVP3018/*tsrA*-2	GATTTCTTTTATTGCTTGTTTAGATAAG CCAGCAGAGCCATTTCATACGTGGTTA ACGACATTAC	
dVP3018/*tsrA*-3	GTAATGTCGTTAACCACGTATGAAATG GCTCTGCTGGCTTATCTAAACAAGCAA TAAAAGAAATC	
dVP3018/*tsrA*-4	GGCTGCAGCTGATTAGCCGCTACGAC GAATACAC	
dc*tsrA*-F	TGGTTTGGCATTAACGCGGTCATC	For checking the deletion of *tsrA* locus in genome
dc*tsrA*-R	ACCGCGTAAGGAGGATACGATGACAG	
ups300-*tsrA*-F BamHI	GGGGATCCAACCATTCGGTGATAAAG CGGGCACAG	For construction of p*tsrA*
tsrA-R SalI	GGGTCGACTTATTGCTTGTTTAGATAA GCCAGCAGTTCATCCGC	

Primers	**Sequence (5' to 3')**	**Description**
ups300-*tsrA*-F BamHI *tsrA*-6xHis-R	GGGGATCCAACCATTCGGTGATAAAG CGGGCACAG GGGTCGACTTAATGGTGATGGTGATG GTGTTGCTTGTTTAGATAAGCCAGCAG TTCATCCGC	For construction of p*tsrA*-6H
ups300-*tsrA*-F BamHI *tsrA*-dC-6xHis-R SalI	GGGGATCCAACCATTCGGTGATAAAG CGGGCACA GGGTCGACTTAATGGTGATGGTGATG GTGCTCGCCCTTGCGTGACTCAATCAC	For construction of p*tsrA*Δ*C*-6H
tsrA-F-NcoI *tsrA*-6xHis-R	CCATGGATGTCGTTAACCACGTATGA AATGGCTCG GGGTCGACTTAATGGTGATGGTGATG GTGTTGCTTGTTTAGATAAGCCAGCAG TTCATCCGC	For construction of pET28a-*tsrA*-6H
hns-3F (pET28a)-F *hns*-3F (pET28a)-R	GTTTAACTTTAAGAAGGAGATATACC ATGTCAGAGCTGACTAAAACAC GCAAGCTTGTCGACCTACTTGTCATCG TCATCCTTG	For construction of p*hns*-3F
pE-SUMO-*hns*-F *hns*-3F (pET28a)-R	GGGGTCTCAAGGTATGTCAGAGCTGA CTAAAACACTTC GCAAGCTTGTCGACCTACTTGTCA TCGTCATCCTTG	For purification of *hns*-3F (construction of pE-SUMO-*hns*-3F)

Primers	Sequence (5' to 3')	Description
pSA19-*tsrA* Q69A F	GAGTCACGCAAGGGCGAGGCAGTTGA GCTATTAGCAAAAGAC	For single amino acid mutation of *tsrA*, Q69A
pSA19-*tsrA* Q69A R	GTCTTTTGCTAATAGCTCAACTGCCTC GCCCTTGCGTGACTC	
pSA19-*tsrA* V70A F	TCACGCAAGGGCGAGCAAGCTGAGCT ATT AGCA	For single amino acid mutation of *tsrA*, V70A
pSA19-*tsrA* V70A R	TGCTAATAGCTCAGCTTGCTCGCCCTT GCG TGA	
pSA19-*tsrA* E71A F	CGCAAGGGCGAGCAAGTTGCGCTATT AGCAAAAGACCTC	For single amino acid mutation of *tsrA*, E71A
pSA19-*tsrA* E71A R	GAGGTCTTTTGCTAATAGCGCAACTTG CTCGCCCTTGCG	
pSA19-*tsrA* L72A F	CGCAAGGGCGAGCAAGTTGAGGCATT AGCAAAAGACCTCGCA	For single amino acid mutation of *tsrA*, L72A
pSA19-*tsrA* L72A R	TGCGAGGTCTTTTGCTAATGCCTCAAC TTGCTCGCCCTTGCG	
pSA19-*tsrA* L73A F	AAGGGCGAGCAAGTTGAGCTAGCAGC AAAAGACCTCGCA	For single amino acid mutation of *tsrA*, L73A
pSA19-*tsrA* L73A R	TGCGAGGTCTTTTGCTGCTAGCTCAAC TTGCTCGCCCTT	
pSA19-*tsrA* A74S F	GGCGAGCAAGTTGAGCTATTAAGCAA AGACCTCGCACAACAAGGT	For single amino acid mutation of *tsrA*, A74S
pSA19-*tsrA* A74S R	ACCTTGTTGTGCGAGGTCTTTGCTTAA TAGCTCAACTTGCTCGCC	

Primers	Sequence (5' to 3')	Description
pSA19-*tsrA* K75A F	GGCGAGCAAGTTGAGCTATTAGCAGC	For single amino
	AGACCTCGCACAACAA	acid mutation of
pSA19-*tsrA* K75A R	TTGTTGTGCGAGGTCTGCTGCTAATAG	*tsrA*, K75A
	CTCAACTTGCTCGCC	
pSA19-*tsrA* D76A F	GGCGAGCAAGTTGAGCTATTAGCAAA	For single amino
	AGCCCTCGCACAACAAGGT	acid mutation of
pSA19-*tsrA* D76A R	ACCTTGTTGTGCGAGGGCTTTTGCTAA	*tsrA*, D76A
	TAGCTCAACTTGCTCGCC	
pSA19-*tsrA* L77A F	GAGCTATTAGCAAAAGACGCCGCACA	For single amino
	ACAAGGTATCTCAGCG	acid mutation of
pSA19-*tsrA* L77A R	CGCTGAGATACCTTGTTGTGCGGCGTC	*tsrA*, L77A
	TTTTGCTAATAGCTC	
pSA19-*tsrA* A78S F	GCAAAAGACCTCAGCCAACAAGGTAT	For single amino
	CTCAGCGGATGAACTGCTG	acid mutation of
pSA19-*tsrA* A78S R	CAGCAGTTCATCCGCTGAGATACCTTG	*tsrA*, A78S
	TTGGCTGAGGTCTTTTGC	
pSA19-*tsrA* Q79A F	GAGCTATTAGCAAAAGACCTCGCAGC	For single amino
	ACAAGGTATCTCAGCG	acid mutation of
pSA19-tsrA Q79A R	CGCTGAGATACCTTGTGCTGCGAGGT	*tsrA*, Q79A
	CTTTTGCTAATAGCTC	
pSA19-*tsrA*	GAGCTATTAGCAAAAGACCTCGCACA	For single amino
Q80A F	AGCAGGTATCTCAGCGGAT	acid mutation of
pSA19-*tsrA*	ATCCGCTGAGATACCTGCTTGTGCGA	*tsrA*, Q80A
Q80A R	GGTCTTTTGCTAATAGCTC	

Primers	Sequence (5' to 3')	Description
pSA19-*tsrA* G81A F	GCAAAAGACCTCGCACAACAAGCTAT CTCAGCGGATGAA	For single amino acid mutation of *tsrA*, G81A
pSA19-*tsrA* G81A R	TTCATCCGCTGAGATAGCTTGTTGTGC GAGGTCTTTTGC	
pSA19-*tsrA* I82A F	GCAAAAGACCTCGCACAACAAGGTGC CTCAGCGGATGAACTG	For single amino acid mutation of *tsrA*, I82A
pSA19-*tsrA* I82A R	CAGTTCATCCGCTGAGGCACCTTGTTG TGCGAGGTCTTTTGC	
pSA19-*tsrA* S83A F	CTCGCACAACAAGGTATCGCAGCGGA TGAACTGCTG	For single amino acid mutation of *tsrA*, S83A
pSA19-*tsrA* S83A R	CAGCAGTTCATCCGCTGCGATACCTTG TTGTGCGAG	
pSA19-*tsrA* A84S F	GACCTCGCACAACAAGGTATCTCAAG CGATGAACTGCTGGCTTATC	For single amino acid mutation of *tsrA*, A84S
pSA19-*tsrA* A84S R	GATAAGCCAGCAGTTCATCGCTTGAG ATACCTTGTTGTGCGAGGTC	
pSA19-*tsrA* D85A F	CAAGGTATCTCAGCGGCAGAACTGCT GGCTTATCTA	For single amino acid mutation of *tsrA*, D85A
pSA19-*tsrA* D85A R	TAGATAAGCCAGCAGTTCTGCCGCTG AGATACCTTG	
pSA19-*tsrA* E86A F	GGTATCTCAGCGGATGCACTGCTGGC TTATCTAAAC	For single amino acid mutation of *tsrA*, E86A
pSA19-*tsrA* E86A R	GTTTAGATAAGCCAGCAGTGCATCCG CTGAGATACC	

Primers	Sequence (5' to 3')	Description
pSA19-*tsrA* L87A F	CAAGGTATCTCAGCGGATGAAGCGCT GGCTTATCTAAACAAGCAA	For single amino acid mutation of *tsrA*, L87A
pSA19-*tsrA* L87A R	TTGCTTGTTTAGATAAGCCAGCGCTTC ATCCGCTGAGATACCTTG	
pSA19-*tsrA* L88A F	GGTATCTCAGCGGATGAACTGGCGGC TTATCTAAACAAGCAA	For single amino acid mutation of *tsrA*, L88A
pSA19-*tsrA* L88A R	TTGCTTGTTTAGATAAGCCGCCAGTTC ATCCGCTGAGATACC	
pSA19-*tsrA* A89S F	GGTATCTCAGCGGATGAACTGCTGAG TTATCTAAACAAGCAACAC	For single amino acid mutation of *tsrA*, A89S
pSA19-*tsrA* A89S R	GTGTTGCTTGTTTAGATAACTCAGCAG TTCATCCGCTGAGATACC	
pSA19-*tsrA* Y90A F	GCGGATGAACTGCTGGCTGCTCTAAA CAAGCAACACCAT	For single amino acid mutation of *tsrA*, Y90A
pSA19-*tsrA* Y90A R	ATGGTGTTGCTTGTTTAGAGCAGCCAG CAGTTCATCCGC	
pSA19-*tsrA* L91A F	GCGGATGAACTGCTGGCTTATGCAAA CAAGCAACACCATCAC	For single amino acid mutation of *tsrA*, L91A
pSA19-*tsrA* L91A R	GTGATGGTGTTGCTTGTTTGCATAAGC CAGCAGTTCATCCGC	
pSA19-*tsrA* N92A F	GAACTGCTGGCTTATCTAGCCAAGCA ACACCATCACCATCAC	For single amino acid mutation of *tsrA*, N92A
pSA19-*tsrA* N92A R	GTGATGGTGATGGTGTTGCTTGGCTAG ATAAGCCAGCAGTTC	

Primers	**Sequence (5’ to 3’)**	**Description**
pSA19-*tsrA* K93A F	CTGCTGGCTTATCTAAACGCGCAACAC CATCACCATCAC	For single amino acid mutation of *tsrA*, K93A
pSA19-*tsrA* K93A R	GTGATGGTGATGGTGTTGCGCGTTTAG ATAAGCCAGCAG	
pSA19-*tsrA* Q94A F	CTGCTGGCTTATCTAAACAAGGCACAC CATCACCATCACCAT	For single amino acid mutation of *tsrA*, Q94A
pSA19-tsrA Q94A R	ATGGTGATGGTGATGGTGTGCCTTGTT TAGATAAGCCAGCAG	

CHAPTER 3

RESULTS

3.1 TsrA negatively affects T3SS2 gene expression

To investigate whether TsrA affects T3SS2 gene expression in *V. parahaemolyticus*, I first constructed a *tsrA* (*VP3018*)-deleted strain derived from the *V. parahaemolyticus* reference strain RIMD2210633 (Δ*tsrA*) and examined the secretion of T3SS2-related proteins into the culture supernatant to monitor the secretory activity of T3SS2 (Figure 8A). In the wild-type (WT) strain, VopD2, VopB2, and VopW, components of the T3SS2 translocon complex, were clearly detected among the T3SS2-secreted proteins. Notably, the secretion of T3SS2-related proteins was further increased in Δ*tsrA* compared to that in WT, indicating that deletion of *tsrA* leads to the hypersecretion of T3SS2. Given the pivotal roles of VtrA and VtrB in T3SS2 gene expression, I examined their expression by immunoblotting. The production of VtrB was increased in Δ*tsrA* compared to that in WT, whereas the protein level of VtrA was rather decreased in Δ*tsrA* compared to that in WT. Considering the hierarchical relationship between VtrA and VtrB, the elevated expression of VtrB likely accounts for the enhanced T3SS2 expression, despite the reduced level of VtrA. In addition, deletion of *vtrB* in the Δ*tsrA* mutant abolished the reduction in VtrA levels**,** suggesting that this decrease is mediated by VtrB activation (Figure 9). Complementation of Δ*tsrA* with a plasmid-borne *tsrA* gene abolished the increased expression of VtrB and the hypersecretion of T3SS2 (Figure 8B). Consistent with the protein production and secretion analyses, transcriptome profiling using RNA-seq showed that the expression of T3SS2-related genes was upregulated in the Δ*tsrA* strain compared to that in the WT strain (Figure 8C). Among the known T3SS2 regulators, only *vtrB* showed an increased expression. These results indicate that TsrA negatively regulates T3SS2 gene expression by modulating *vtrB* expression.

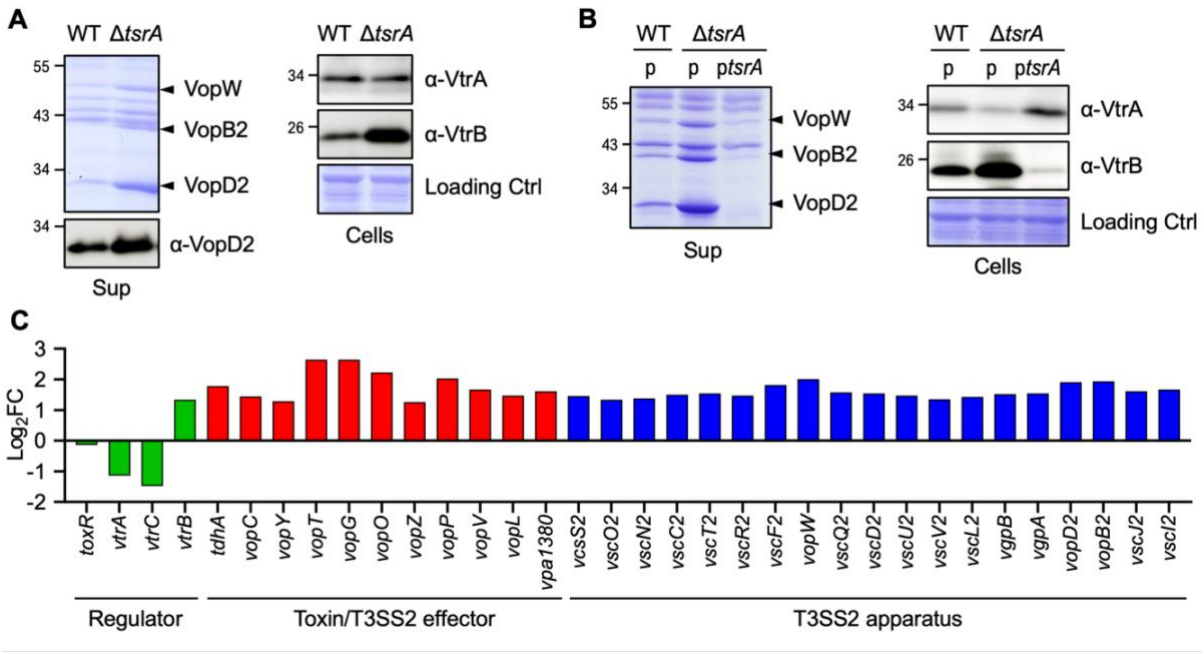


Fig 8. TsrA negatively affects the expression of T3SS2 genes.

(A) The *tsrA*-deleted strain (Δ*tsrA*) showed increased levels of T3SS2-related proteins. *V. parahaemolyticus* WT and Δ*tsrA* strains were grown in LB medium at 37°C to an OD_{600} of 1.8. Secreted proteins in culture supernatants (Sup) were analyzed by SDS-PAGE followed by CBB staining, with T3SS2-secreted proteins (VopW, VopB2, and VopD2) indicated by arrowheads, or by immunoblotting for VopD2. Bacterial cell lysates (Cells) were analyzed by immunoblotting for VtrA and VtrB, with proteins visualized by CBB staining serving as a loading control. (B) Complementation of *tsrA* gene restored the repressive effect on T3SS2-related proteins. *V. parahaemolyticus* WT and Δ*tsrA* strains harboring pSA19 empty vector (indicated as p), and Δ*tsrA* harboring pSA19-*tsrA* with the endogenous promoter (indicated as p*tsrA*) were grown in LB medium at 37°C to an OD_{600} of 1.8. Sup was separated by SDS-PAGE, followed by CBB staining, and Cells were analyzed by immunoblotting for VtrA and VtrB. Cell lysate proteins visualized by CBB staining served as a loading control. (C) Differentially expressed genes related to T3SS2 in the Δ*tsrA* mutant compared to the WT strain. Total RNA was extracted from *V. parahaemolyticus* WT and Δ*tsrA* strains grown in LB medium at 37°C to an OD_{600} of 0.8–1.0 and analyzed using RNA-Seq.

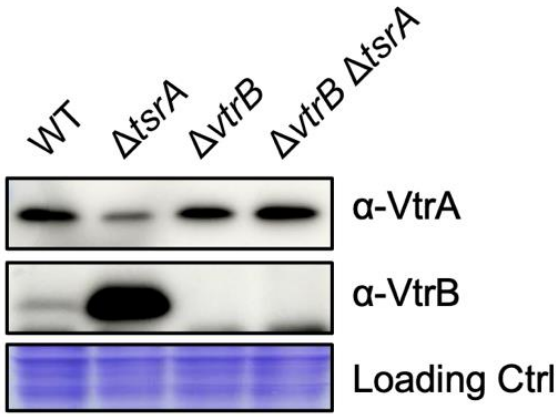


Fig 9. VtrA reduction in Δ*tsrA* is mediated by VtrB.

V. parahaemolyticus strains WT, Δ*tsrA*, Δ*vtrB*, and Δ*vtrB* Δ*tsrA* were grown in LB medium at 37°C to an OD_{600} of 1.8. Bacterial cell lysates were analyzed by immunoblotting for VtrA and VtrB, with proteins visualized by CBB staining serving as a loading control.

3.2 TsrA affects primary activation of *vtrB* gene expression

Prior study showed that *vtrB* gene expression is conferred by a two-step transcriptional activation, in which VtrA-mediated primary activation of *vtrB* transcription from the *vtrB* promoter is followed by secondary activation by VtrB-mediated read-through transcription from the operon upstream of *vtrB* (12). To dissect the mechanisms by which TsrA affects *vtrB* gene expression, I performed a time-course northern blot analysis of *vtrB* transcripts using a probe against the *vtrB* promoter (Figure 10A). RNA was collected at multiple time points following a temperature shift from 25°C (non-permissive for *vtrB* expression) to 37°C (permissive for *vtrB* expression). In the WT strain, the S transcript of ~700 nt from the *vtrB* promoter, derived from primary activation, appeared 15 min post-induction. The ~4000-nt L and ~2,000-nt M transcripts generated by secondary activation via read-through transcription of the operon upstream of *vtrB* were detected 30 min after induction. In the Δ*tsrA* strain, increased levels of the S transcript were observed at 15 min post-induction and L/M transcripts

from 30 min post-induction. I also measured *vtrB* transcript levels by quantitative real-time PCR (qRT-PCR) targeting the 5'-untranslated region of the *vtrB* gene to quantitatively compare *vtrB* expression in each strain. The *vtrB* transcript was significantly increased in the Δ*tsrA* strain compared to that in the WT strain 15 min post-induction (Figure 10B).

To further determine whether TsrA affects primary or secondary activation of *vtrB* gene expression, I tested the effect of *tsrA* deletion on *vtrB* gene expression over time by northern blotting with the *vtrB*-deleted strain (Δ*vtrB*) lacking secondary activation, as a background (Figure 10A). In the Δ*vtrB* strain, a ~200-nt *vtrB* transcript with a deletion in the *vtrB* coding sequence was detected 15 min after induction. The *tsrA*-deleted strain derived from the Δ*vtrB* strain (Δ*vtrB* Δ*tsrA*) showed increased *vtrB* transcript levels. Consistent with this, qRT-PCR analysis also indicated the upregulation of *vtrB* transcripts in the Δ*vtrB* Δ*tsrA* strain compared to that in the Δ*vtrB* strain (Figure 10B). Collectively, these results indicate that TsrA affects *vtrB* expression during primary activation.

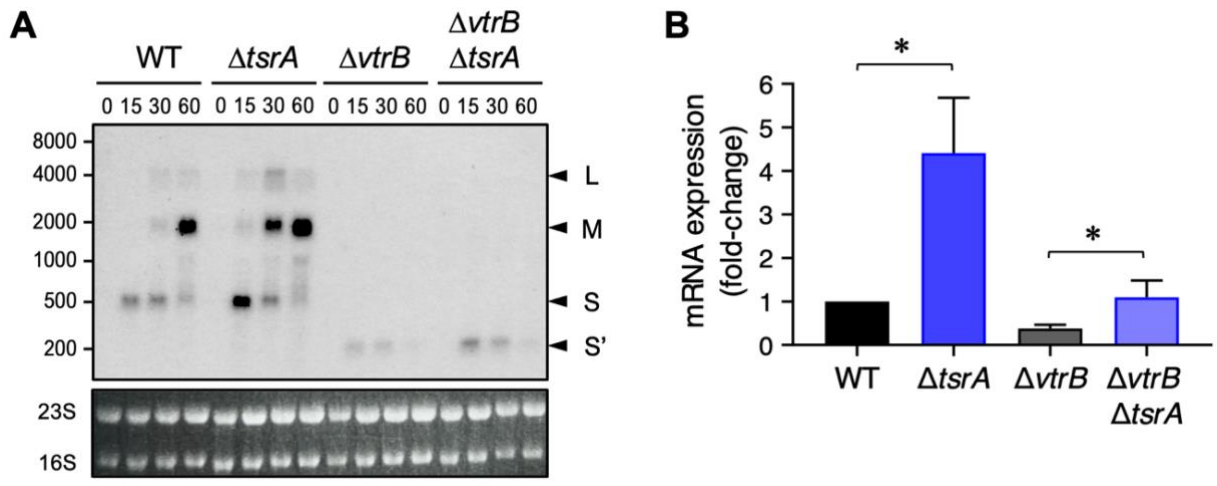


Fig 10. TsrA affects the initial activation of *vtrB* transcription.

(A) Time-course analysis of *vtrB* transcripts in *V. parahaemolyticus* strains. The indicated strains were grown to an OD_{600} of 0.8 at 25°C, a non-permissive condition for *vtrB* expression, and then shifted to 37°C to induce *vtrB* gene expression. RNA was extracted at 0, 15, 30, and 60 min after induction, and northern blotting was performed using a P_{vtrB} probe. L, 4,000-nt L

transcript; M, 2,000-nt M transcript; S, 700-nt S transcript; S', S transcript containing *vtrB* deletion. 23S rRNA and 16S rRNA were used as loading controls. (B) Relative expression of the *vtrB* promoter region in *V. parahaemolyticus* WT, Δ*tsrA*, Δ*vtrB*, and Δ*vtrB* Δ*tsrA* strains. Total RNA samples collected 15 min after induction in panel A were used for qRT-PCR analysis. Expression levels were normalized to *recA* and expressed relative to those of the WT strain. *, $p < 0.01$ by Student's t-test.

3.3 TsrA negatively affects T3SS2-dependent virulence

Given that T3SS2 plays a crucial role in the pathogenicity of *V. parahaemolyticus*, including cytotoxicity and enterotoxicity (8), I investigated whether TsrA affects T3SS2-mediated virulence. *V. parahaemolyticus* exhibits T3SS2-dependent cytotoxicity in human colon adenocarcinoma Caco-2 cells. To exclude cytotoxicity depending on other factors, such as type III secretion system 1 (T3SS1) and thermostable direct hemolysin (TDH), a T3SS1- and TDH-defective strain POR-2, was used as a background. Caco-2 cells were infected with *V. parahaemolyticus* POR-2 strain or its derivative, the *tsrA*-deleted strain (POR-2 Δ*tsrA*), and cytotoxicity was evaluated (Figure 11A). Notably, POR-2 Δ*tsrA* was significantly more cytotoxic than the parental POR-2 strain, causing complete cell death 4.5 h after infection, and this higher cytotoxicity was attenuated by plasmid-mediated complementation of *tsrA*.

Diarrhea-inducing activity is an important virulence trait of *V. parahaemolyticus* mediated by T3SS2. Therefore, I investigated the effect of TsrA on the diarrhea-inducing activity of *V. parahaemolyticus* in the rabbit ileal loop model, in which *V. parahaemolyticus* strains were inoculated into the ligated ileal loops of rabbits, and fluid accumulation in each loop was measured 16 h after infection. The Δ*tsrA* strain induced significantly increased fluid accumulation in rabbit ileal loops compared to the parental strain POR-2 (Figure 11B). These results indicate that TsrA suppresses T3SS2-mediated pathogenicity.

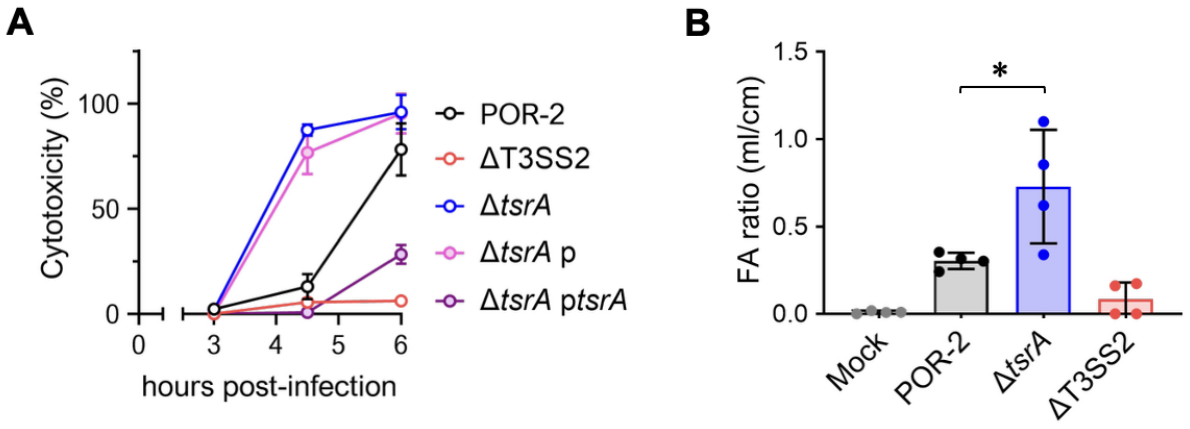


Fig 11. TsrA negatively affects the T3SS2-dependent virulence.

(A) Time-course analysis of the cytotoxicity of Caco-2 cells infected with the indicated *V. parahaemolyticus* strains at a multiplicity of infection of 10. Cytotoxicity was evaluated by measuring lactate dehydrogenase release. Data are represented as mean ± SD (n=3). (B) Fluid accumulation induced by the indicated *V. parahaemolyticus* strains was analyzed using the rabbit ileal loop model. Each ligated loop was infected with bacteria (POR2 and Δ*tsrA*: 10^8 CFU; ΔT3SS2: 10^9 CFU) or was uninfected, and fluid accumulation in the loop was evaluated 16 h post-infection. The FA ratio represents the amount of accumulated fluid (ml) per length (cm) of the ligated small intestine. Data are represented as mean ± SD (n=4). *, $p < 0.01$ by Student's t-test.

3.4 TsrA interacts with H-NS

I then aimed to address the repressive mechanisms of TsrA on *vtrB* expression. Given that TsrA lacks a DNA-binding motif for the direct regulation of transcription, I hypothesized that TsrA interacts with other factors to repress *vtrB* transcription. To identify *V. parahaemolyticus* proteins that interact with TsrA, C-terminally 6×His-tagged TsrA (TsrA-6×His) expressed in *Escherichia coli* was immobilized on Ni-NTA beads and incubated with *V. parahaemolyticus* lysates. Proteins bound to TsrA were separated by SDS-PAGE, followed

by Coomassie Brilliant Blue (CBB) staining, and a protein of ~17 kDa was found to be specifically associated with TsrA (Figure 12A). The protein band was subjected to liquid chromatography-tandem mass spectrometry (LC-MS/MS) analysis and was subsequently identified as H-NS. I also subjected purified 3×FLAG-tagged H-NS protein (H-NS-3×FLAG) to Ni-NTA beads immobilized with TsrA-6×His, which exhibited direct binding between TsrA and H-NS (Figure 13). Furthermore, co-immunoprecipitation from the lysate of a *V. parahaemolyticus* strain co-expressing H-NS-3×FLAG and TsrA-6×His revealed that TsrA co-precipitated with H-NS, confirming their *in vivo* interaction (Figure 12B). These results indicate that TsrA interacts with H-NS.

To gain insight into the structural basis of this interaction, I performed structural modeling using AlphaFold3, which suggested that the C-terminal region of TsrA interacts with the N-terminal dimerization domain of H-NS (Figure 15). To determine whether the C-terminal region of TsrA is required for binding to H-NS, I constructed a truncated TsrA mutant lacking the C-terminal region (residues 1–68, TsrAΔC) and evaluated its binding activity. TsrA-6×His or TsrAΔC-6×His protein expressed in *E. coli* was immobilized on Ni-NTA beads, and its interaction with purified 3×FLAG-tagged H-NS was examined. In contrast to full-length TsrA, TsrAΔC did not interact with H-NS (Figure 12C). Furthermore, complementation of the Δ*tsrA* strain with *tsrA*-6×His (Δ*tsrA* p*tsrA*-6H) abolished the increased expression of VtrB and hypersecretion of T3SS2, whereas the expression of *tsrA*ΔC-6×His in the Δ*tsrA* strain (Δ*tsrA* p*tsrA*ΔC-6H) did not restore these phenotypes (Figure 12D). To further characterize the interaction between TsrA and H-NS, I performed Ala/Ser scanning mutagenesis of the C-terminal region of TsrA (residues 69–94). A series of p*tsrA*-6H derivatives were expressed in the Δ*tsrA* strain, and VtrB production and VopD2 secretion were assessed. Among the 26 mutants, I82A, L87A, and L91A showed higher levels of VtrB production and VopD2 secretion than wild-type TsrA (Figure 14), indicating that these residues contribute to the

regulatory activity of TsrA, possibly by mediating its interaction with H-NS. This notion is supported by the AlphaFold3 structural model, in which these residues were predicted to be positioned at the interface with H-NS (Figure 15). Collectively, these results indicate that the C-terminal region of TsrA mediates its interaction with H-NS, which is critical for negative regulation of T3SS2.

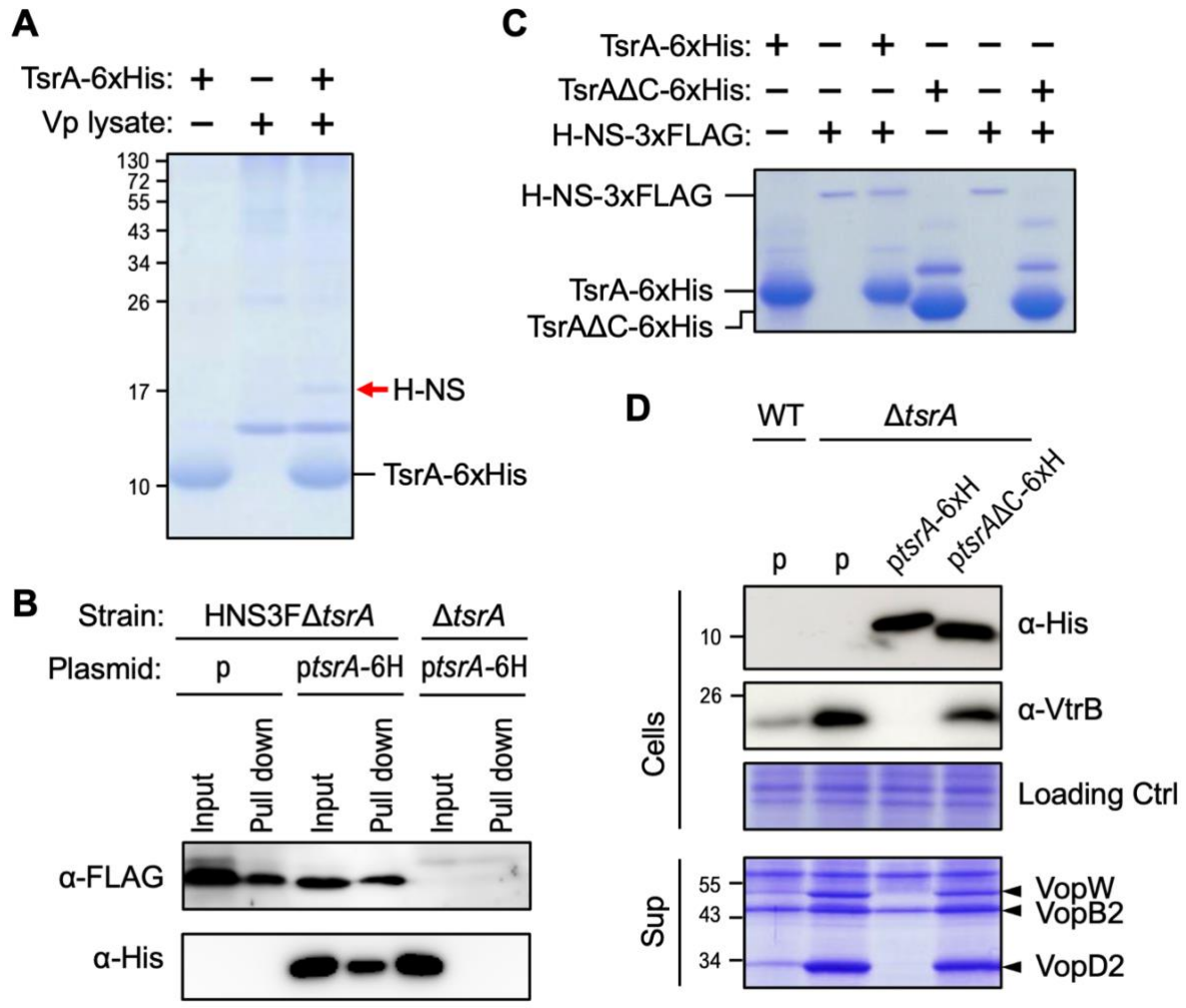


Fig 12. TsrA interacts with H-NS.

(A) TsrA-interacting proteins were purified from *V. parahaemolyticus* lysates using a TsrA-6×His-immobilized Ni-NTA column. Bound proteins were separated by SDS-PAGE and visualized by CBB staining. The arrow indicates H-NS. (B) FLAG co-immunoprecipitation from lysates of the HNS-3F Δ*tsrA* strain harboring either p*tsrA*–6H (encoding TsrA-6×His) or

an empty vector, and from the Δ*tsrA* strain harboring p*tsrA*–6H. Bound proteins were eluted and analyzed by immunoblotting using anti-FLAG or anti-His antibodies. (C) Binding of H-NS to TsrA or TsrAΔC. TsrA-6×His or TsrAΔC-6×His was immobilized on a Ni-NTA column, and purified H-NS-3×FLAG was applied. The eluates were analyzed by SDS-PAGE and visualized by CBB staining. (D) The C-terminal region of TsrA is required for the repression of VtrB production and T3SS2 secretion. *V. parahaemolyticus* WT and Δ*tsrA* strains carrying an empty vector (p), or Δ*tsrA* complemented with p*tsrA*-6H or p*tsrA*ΔC-6H were grown in LB medium at 37 °C to an OD_{600} of 1.8. Cell lysates (Cells) were subjected to immunoblotting with the indicated antibodies, with CBB-stained proteins serving as the loading control. Culture supernatants (Sup) were analyzed by SDS-PAGE and CBB staining. T3SS2-secreted proteins (VopW, VopB2, and VopD2) are marked by arrowheads.

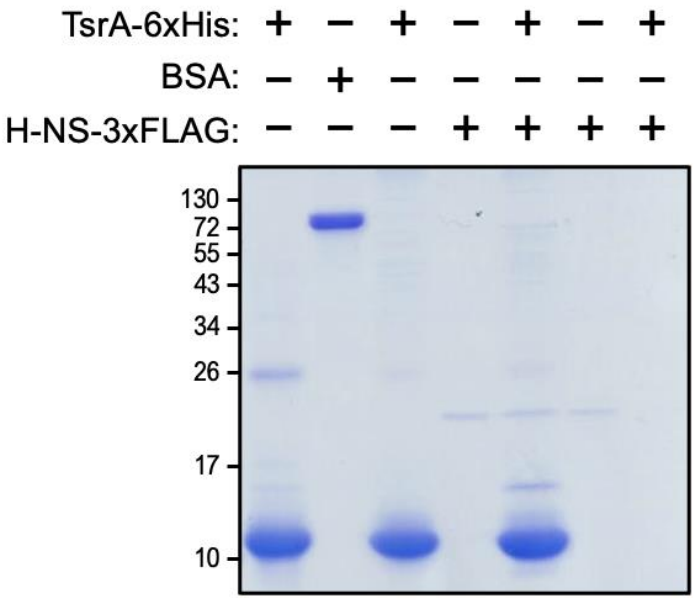


Fig 13. TsrA directly interact with H-NS (comparison with BSA as negative control).

Ni-NTA beads immobilized with TsrA-6×His protein or control beads were incubated with purified H-NS-3×FLAG protein or bovine serum albumin (BSA). The eluates were analyzed by SDS-PAGE, followed by CBB staining.

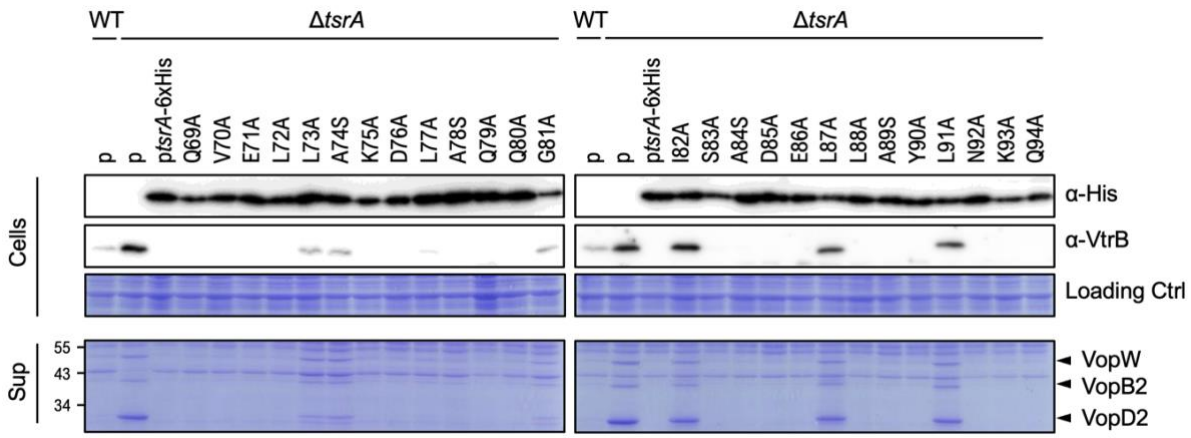


Fig 14. Mutational analysis of the C-terminal region of TsrA.

V. parahaemolyticus WT harboring an empty vector (p), and the Δ*tsrA* strain carrying either an empty vector, p*tsrA*-6H, or p*tsrA*-6H derivatives containing Ala/Ser substitutions in the C-terminal region (residues 69–94) were grown in LB medium at 37 °C to an OD600 of 1.8. Culture supernatants (Sup) were analyzed by SDS-PAGE, followed by CBB staining. Whole-cell lysates (Cells) were subjected to immunoblotting with anti-VtrB and anti-His antibodies, with CBB-stained proteins serving as a loading control. An asterisk indicates a nonspecific background band.

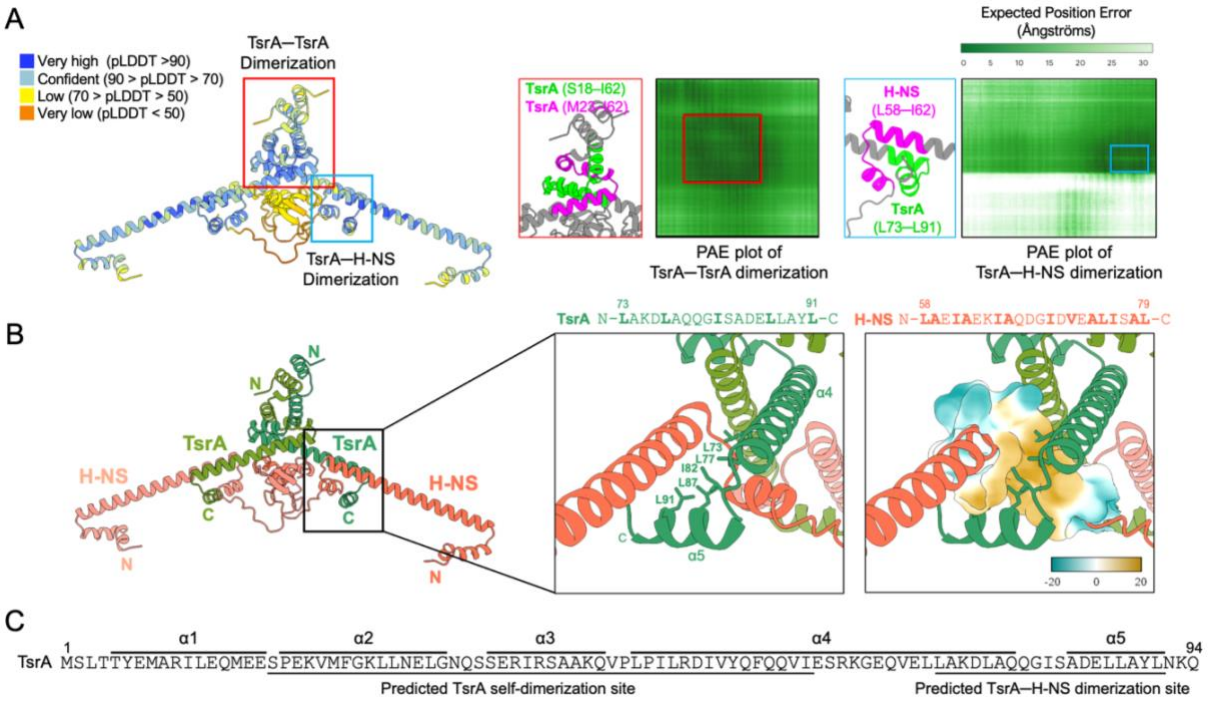


Fig 15. Structural modeling of the TsrA–H-NS complex predicted by AlphaFold3.

(A) Predicted heteromeric structure of H-NS/TsrA at 2:2 ratio, colored by pLDDT score with PAE plot showing a high confidence level (dark green) between TsrA–TsrA and TsrA–H-NS interfaces. The TsrA–TsrA dimerization has been suggested in *V. cholerae* by Caro *et al.* (2020) and Rakibova *et. al.* (2024) , aligned with my structural prediction. (B) The H-NS–TsrA complex with close-up view of the interaction interface. TsrA dimer acts as a bridge between two H-NS monomers. Residues of TsrA critical for its repressive activity, identified through the Ala/Ser mutational analysis in Fig 5, are indicated. These residues may interact with the hydrophobic surfaces of H-NS. Residues involved in hydrophobic interactions are in bold letters. The proteins were colored according to their polypeptide chains. (C) Amino acid sequence and predicted secondary structure of TsrA.

CHAPTER 4

DISCUSSION

Pathogenic bacteria rely on precise regulation of virulence gene expression to ensure survival and adaptation in diverse environments. In *V. parahaemolyticus*, T3SS2 is a major virulence determinant, and its activity is governed by regulatory circuits that integrate environmental cues (13, 38). Here, I identified TsrA as a negative regulator of T3SS2 gene expression, thereby uncovering a previously unrecognized layer in the regulatory network of *V. parahaemolyticus*. This regulation is achieved by modulating the expression of VtrB, a transcriptional activator essential for T3SS2 expression. The transcription of *vtrB* is primarily driven by the VtrA/VtrC complex and secondarily amplified through read-through transcription from the upstream *VPA1356–VPA1349* operon (10, 12, 39). My findings indicate that the negative effect of TsrA acts specifically on the primary activation step of *vtrB* expression (Figure 10), without increasing the expression of the initial activators (Figure 8C). This mechanism likely functions to restrict *vtrB* expression levels, suggesting that TsrA plays a crucial role in controlling the amplification of *vtrB* expression.

The absence of a putative DNA-binding domain in TsrA suggests that its function is mediated not by direct DNA recognition, but by interactions with other regulatory factors. I found that TsrA interacts with H-NS (Figure 12), a nucleoid-associated protein extensively studied in organisms such as *Escherichia coli* and *Salmonella enterica*, where it often cooperates with co-regulators such as StpA and Hha to modulate repression strength and gene specificity (22, 40). My results suggest that TsrA may act as an H-NS co-regulator in *V. parahaemolyticus*, thereby expanding the repertoire of known H-NS-associated modulators. This is reminiscent of observations in *V. cholerae*, where TsrA is implicated in a functional association with H-NS, with a structural model predicting its interaction (25, 26). Nevertheless,

to my knowledge, my data provide the first experimental evidence of TsrA-H-NS interactions. Structural modeling using AlphaFold3 predicted that the C-terminal region of TsrA interacts with the N-terminal oligomerization domain of H-NS (Figure 15). Notably, a TsrA variant lacking the C-terminal region (residues 69–94) failed to interact with H-NS and lost its ability to repress *vtrB* expression and T3SS2 secretion (Figures 12C and 12D). In addition, the Ala/Ser scanning analysis identified several residues in the C-terminal region of TsrA that are important for repressive activity. These residues are hydrophobic amino acids and are predicted, in the AlphaFold3 model, to interact with hydrophobic residues within the site 2 dimerization region of H-NS, potentially forming an interlocking between TsrA and H-NS through hydrophobic interactions (Figures 14 and 15B). These observations suggest that the interaction with H-NS underlies the regulatory activity of TsrA, and that TsrA may mimic or complement H-NS structural motifs to facilitate complex formation. Several studies have shown that H-NS exerts its repressive activity through its ability to oligomerize along DNA, forming linear and/or bridged nucleoprotein filaments (41). These filaments prevent RNA polymerase (RNAP) from initiating transcription at promoters, halt its elongation, and trap it within DNA loops (42). Well-known H-NS co-regulators, such as StpA and Hha-like proteins, interact with H-NS via its dimerization domain (43, 44). Among these co-regulators, TsrA shares a feature with Hha-like proteins in that it lacks a DNA-binding domain. Hha binds symmetrically to the site 1 dimerization region of H-NS at a 1:1 ratio, exposing a positively charged surface that enhances H-NS binding to DNA (22, 45). The interaction between Hha and H-NS stimulates DNA-DNA bridging activity and increases RNAP pausing (40). In contrast to Hha, the predicted model suggests that TsrA dimerizes via its N-terminal region, with each C-terminal domain engaging the site 2 dimerization region of H-NS, bridging two H-NS monomers without creating an exposed positively charged surface. Here, when an N-terminal deletion variant of His-tagged TsrA (1–68) was expressed from a plasmid in *V. parahaemolyticus*, no expression was detected

(data not shown), suggesting that the predicted N-terminal dimerization domain may contribute to the stability of TsrA. These observations suggest that TsrA operates mechanistically differently from Hha, likely contributing to the stabilization of H-NS nucleoprotein filament complexes and modulating their activity rather than directly facilitating H-NS filament–DNA binding. A deeper mechanistic understanding of how TsrA modulates H-NS activity warrants further exploration in future studies.

The distribution of Hha-like proteins is restricted to *Enterobacteriaceae* (46), whereas TsrA is found in *Vibrionaceae* (23, 25). This evolutionary distinction may reflect the mechanistic differences between TsrA and Hha as H-NS co-regulators of gene expression. The notion that TsrA functions as an H-NS co-regulator is also supported by my observation in the H-NS–TsrA double mutant (Figure 16). Interestingly, under the permissive condition for T3SS2 expression, the *hns* mutant does not exhibit increased expression of *vtrB* or T3SS2 genes relative to the wild-type strain (13), unlike the *tsrA* mutant. Nevertheless, deletion of both *tsrA* and *hns* abolished upregulation of *vtrB* expression and T3SS2 secretion observed in the *tsrA* single mutant. These findings indicate that TsrA-mediated T3SS2 repression is dependent on H-NS. The Vp-PAI region, which harbors the T3SS2 gene cluster, spans approximately 80 kb of AT-rich DNA suitable for H-NS binding (13). In addition to H-NS, bacteria contain a variety of other nucleoid-associated proteins (NAPs) (47–49). For example, *E. coli* HU shows a preference for A/T-rich DNA, similar to H-NS (50). Therefore, it is conceivable that the loss of *hns* could induce partial compensatory silencing of the Vp-PAI locus by other NAPs, potentially masking the H-NS–dependent repression of T3SS2 genes that would otherwise be observed in the absence of TsrA.

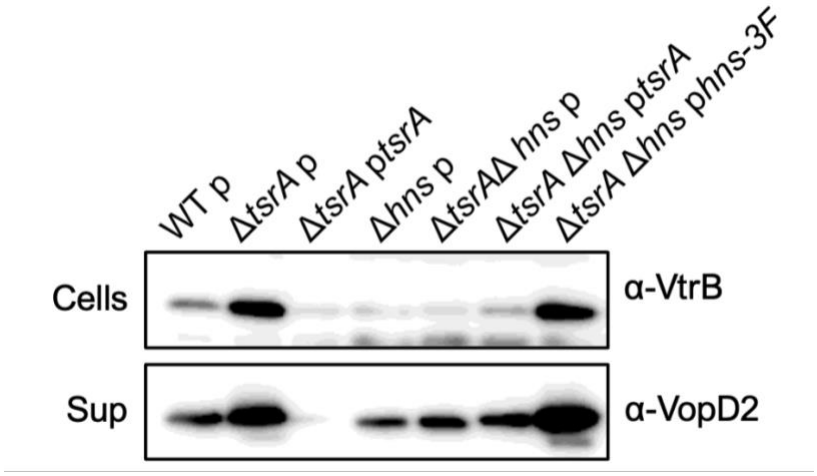


Fig 16. The regulatory activity of TsrA is dependent on H-NS.

The indicated *V. parahaemolyticus* strains were grown in LB medium at 37°C to an OD_{600} of 1.8. Secreted proteins in culture supernatants (Sup) were analyzed by immunoblotting for VopD2, and bacterial cell lysates (Cells) were analyzed by immunoblotting for VtrB. Deletion of *hns* in the *tsrA* mutant (Δ*tsrA* Δ*hns*) abolished the increased expression of VtrB and enhanced T3SS2 secretion observed in Δ*tsrA*, resulting in a phenotype comparable to that of the *hns* mutant (Δ*hns*). This effect was restored by complementation with *hns*, but not with *tsrA* mutation.

CHAPTER 5

CONCLUDING REMARKS

The major foodborne pathogen *V. parahaemolyticus* depends on T3SS2 for intestinal virulence, but the complete picture of the T3SS2 gene regulatory network remains elusive. In this study, I identifies TsrA as a novel virulence repressor in *V. parahaemolyticus*, revealing a mechanism by which this small protein restricts T3SS2 activation through modulating *vtrB* transcription initiation. Moreover, I provide experimental evidence that TsrA interacts with H-NS, highlighting TsrA as an H-NS co-regulator. Although further investigation is warranted to elucidate how TsrA integrates into H-NS–mediated silencing, my findings not only advance the understanding of how virulence regulation is fine-tuned in *V. parahaemolyticus* but also shed light on the evolutionary strategies underlying the xenogeneic silencing of horizontally acquired genes.

REFERENCES

1. Fujino T, Okuno Y, Nakada D, Aoyama A, Fukai K, Mukai T, Ueho T. 1951. On the bacteriological examination of shirasu food poisoning (in Japanese). J Japanese Assoc Infect Dis 25:11.
2. Joseph SW, Colwell RR, Kaper JB. 1982. *Vibrio parahaemolyticus* and Related Halophilic Vibrios. Crit Rev Microbiol 10:77–124.
3. Li L, Meng H, Gu D, Li Y, Jia M. 2019. Molecular mechanisms of *Vibrio parahaemolyticus* pathogenesis. Microbiol Res 222:43–51.
4. Letchumanan V, Chan KG, Lee LH. 2014. *Vibrio parahaemolyticus*: A review on the pathogenesis, prevalence, and advance molecular identification techniques. Front Microbiol 5:1–13.
5. Sugiyama T, Iida T, Izutsu K, Park KS, Honda T. 2008. Precise region and the character of the pathogenicity island in clinical *Vibrio parahaemolyticus* strains. J Bacteriol 190:1835–1837.
6. Makino K, Oshima K, Kurokawa K, Yokoyama K, Uda T, Tagomori K, Iijima Y, Najima M, Nakano M, Yamashita A, Kubota Y, Kimura S, Yasunaga T, Honda T, Shinagawa H, Hattori M, Iida T. 2003. Genome sequence of *Vibrio parahaemolyticus*: A pathogenic mechanism distinct from that of *V. cholerae*. Lancet 361:743–749.
7. Shrestha M, Bernhards RC, Fu Y, Ryan K, Schubot FD. 2020. Backbone Interactions Between Transcriptional Activator ExsA and Anti-Activator ExsD Facilitate Regulation of the Type III Secretion System in *Pseudomonas aeruginosa*. Sci Rep 10:1–8.
8. Hiyoshi H, Kodama T, Iida T, Honda T. 2010. Contribution of *Vibrio parahaemolyticus* virulence factors to cytotoxicity, enterotoxicity, and lethality in mice. Infect Immun 78:1772–1780.

9. Kodama T, Gotoh K, Hiyoshi H, Morita M, Izutsu K, Akeda Y, Park KS, Cantarelli V V., Dryselius R, Iida T, Honda T. 2010. Two regulators of *Vibrio parahaemolyticus* play important roles in enterotoxicity by controlling the expression of genes in the Vp-PAI region. PLoS One 5:e8678.
10. Okada R, Matsuda S, Iida T. 2017. *Vibrio parahaemolyticus* VtrA is a membrane-bound regulator and is activated via oligomerization. PLoS One 12:1–16.
11. Li P, Rivera-Cancel G, Kinch LN, Salomon D, Tomchick DR, Grishin N V., Orth K. 2016. Bile salt receptor complex activates a pathogenic type III secretion system. Elife 5:1–26.
12. Anggramukti DS, Ishii E, Pratama A, Kadi M Al, Iida T, Kodama T, Matsuda S. 2024. The read-through transcription-mediated autoactivation circuit for virulence regulator expression drives robust type III secretion system 2 expression in *Vibrio parahaemolyticus*. PLoS Pathog 20:1–22.
13. Pratama A, Ishii E, Kodama T, Iida T, Matsuda S. 2023. The Xenogeneic Silencer Histone-Like Nucleoid-Structuring Protein Mediates the Temperature and Salinity-Dependent Regulation of the Type III Secretion System 2 in *Vibrio parahaemolyticus*. J Bacteriol 205:e0026622.
14. Abera D. 2021. Regulation of Virulence Gene Expression in Bacteria: A Review. J Biol Agric Healthc 11:9–18.
15. Dorman CJ. 2009. Global regulators and environmental adaptation in Gram-negative pathogens. Clin Microbiol Infect 15:47–50.
16. Dorman CJ. 2007. H-NS, the genome sentinel. Nat Rev Microbiol 5:157–161.
17. Navarre WW, Porwollik S, Wang Y, McClelland M, Rosen H, Libby SJ, Fang FC. 2006. Selective Silencing of Foreign DNA with Low GC Content by the H-NS Protein in *Salmonella*. Science 313:236–238.

18. Dame RT, Wyman C, Goosen N. 2000. H-NS mediated compaction of DNA visualised by atomic force microscopy. Nucleic Acids Res 28:3504–3510.

19. Winardhi RS, Yan J, Kenney LJ. 2015. H-NS Regulates Gene Expression and Compacts the Nucleoid: Insights from Single-Molecule Experiments. Biophys J 109:1321–1329.

20. Dorman CJ, Kane KA. 2009. DNA bridging and antibridging: A role for bacterial nucleoid-associated proteins in regulating the expression of laterally acquired genes. FEMS Microbiol Rev 33:587–592.

21. Lim CJ, Whang YR, Kenney LJ, Yan J. 2012. Gene silencing H-NS paralogue StpA forms a rigid protein filament along DNA that blocks DNA accessibility. Nucleic Acids Res 40:3316–3328.

22. Ali SS, Whitney JC, Stevenson J, Robinson H, Howell PL, Navarre WW. 2013. Structural insights into the regulation of foreign genes in *Salmonella* by the Hha/H-NS complex. J Biol Chem 288:13356–13369.

23. DuPai CD, Cunningham AL, Conrado AR, Wilke CO, Davies BW. 2020. TsrA Regulates Virulence and Intestinal Colonization in *Vibrio cholerae*. mSphere 5:1–8.

24. Zheng J, Shin OS, Cameron DE, Mekalanos JJ. 2010. Quorum sensing and a global regulator TsrA control expression of type VI secretion and virulence in *Vibrio cholerae*. Proc Natl Acad Sci U S A 107:21128–21133.

25. Caro F, Caro JA, Place NM, Mekalanos JJ. 2020. Transcriptional Silencing by TsrA in the Evolution of Pathogenic *Vibrio cholerae* Biotypes. MBio 11:1–14.

26. Rakibova Y, Dunham DT, Seed KD, Freddolino L. 2024. Nucleoid-associated proteins shape the global protein occupancy and transcriptional landscape of a clinical isolate of *Vibrio cholerae*. mSphere 9:e00011-24.

27. Park KS, Ono T, Rokuda M, Jang MH, Okada K, Iida T, Honda T. 2004. Functional characterization of two type III secretion systems of *Vibrio parahaemolyticus*. Infect

Immun 72:6659–6665.

28. Matsuda S, Okada R, Tandhavanant S, Hiyoshi H, Gotoh K, Iida T, Kodama T. 2019. Export of a *Vibrio parahaemolyticus* toxin by the Sec and type III secretion machineries in tandem. Nat Microbiol 4:781–788.

29. Langmead B, Salzberg SL. 2012. Fast gapped-read alignment with Bowtie 2. Nat Methods 9:357–359.

30. Anders S, Pyl PT, Huber W. 2015. HTSeq-A Python framework to work with high-throughput sequencing data. Bioinformatics 31:166–169.

31. Ge SX, Son EW, Yao R. 2018. iDEP: An integrated web application for differential expression and pathway analysis of RNA-Seq data. BMC Bioinformatics 19:1–24.

32. Aiba H, Adhya S, de Crombrugghe B. 1981. Evidence for two functional gal promoters in intact *Escherichia coli* cells. J Biol Chem 256:11905–11910.

33. Abramson J, Adler J, Dunger J, Evans R, Green T, Pritzel A, Ronneberger O, Willmore L, Ballard AJ, Bambrick J, Bodenstein SW, Evans DA, Hung CC, O'Neill M, Reiman D, Tunyasuvunakool K, Wu Z, Žemgulytė A, Arvaniti E, Beattie C, Bertolli O, Bridgland A, Cherepanov A, Congreve M, Cowen-Rivers AI, Cowie A, Figurnov M, Fuchs FB, Gladman H, Jain R, Khan YA, Low CMR, Perlin K, Potapenko A, Savy P, Singh S, Stecula A, Thillaisundaram A, Tong C, Yakneen S, Zhong ED, Zielinski M, Žídek A, Bapst V, Kohli P, Jaderberg M, Hassabis D, Jumper JM. 2024. Accurate structure prediction of biomolecular interactions with AlphaFold 3. Nature 630:493–500.

34. Meng EC, Goddard TD, Pettersen EF, Couch GS, Pearson ZJ, Morris JH, Ferrin TE. 2023. UCSF ChimeraX: Tools for structure building and analysis. Protein Sci 32:1–13.

35. Kodama T, Rokuda M, Park K, Cantarelli V V, Matsuda S, Iida T, Honda T. 2007. Identification and characterization of VopT, a novel ADP-ribosyltransferase effector protein secreted via the *Vibrio parahaemolyticus* type III secretion system 2. Cell

Microbiol 9:2598–2609.

36. Kodama T, Akeda Y, Kono G, Takahashi A, Imura K, Iida T, Honda T. 2002. The EspB protein of enterohaemorrhagic *Escherichia coli* interacts directly with α-catenin. Cell Microbiol 4:213–222.

37. Nomura T, Hamashima H, Okamoto K. 2000. Carboxy terminal region of haemolysin of *Aeromonas sobria* triggers dimerization. Microb Pathog 28:25–36.

38. Gotoh K, Kodama T, Hiyoshi H, Izutsu K, Park KS, Dryselius R, Akeda Y, Honda T, Iida T. 2010. Bile acid-induced virulence gene expression of *Vibrio parahaemolyticus* reveals a novel therapeutic potential for bile acid sequestrants. PLoS One 5:e13365.

39. Li P, Rivera-Cancel G, Kinch LN, Salomon D, Tomchick DR, Grishin N V., Orth K. 2016. Bile salt receptor complex activates a pathogenic type III secretion system. Elife 5:e15718.

40. Boudreau BA, Hron DR, Qin L, Van Der Valk RA, Kotlajich M V., Dame RT, Landick R. 2018. StpA and Hha stimulate pausing by RNA polymerase by promoting DNA-DNA bridging of H-NS filaments. Nucleic Acids Res 46:5525–5546.

41. Lim CJ, Lee SY, Kenney LJ, Yan J. 2012. Nucleoprotein filament formation is the structural basis for bacterial protein H-NS gene silencing. Sci Rep 2:1–6.

42. Hustmyer CM, Landick R. 2024. Bacterial chromatin proteins, transcription, and DNA topology: Inseparable partners in the control of gene expression. Mol Microbiol 122:81–112.

43. Williams RM, Rimsky S, Buc H. 1996. Probing the structure, function, and interactions of the *Escherichia coli* H-NS and StpA proteins by using dominant negative derivatives. J Bacteriol 178:4335–4343.

44. Nieto JM, Madrid C, Prenafeta A, Miquelay E, Balsalobre C, Carrascal M, Juárez A. 2000. Expression of the hemolysin operon in *Escherichia coli* is modulated by a

nucleoid-protein complex that includes the proteins Hha and H-NS. Mol Gen Genet 263:349–358.

45. García J, Madrid C, Juárez A, Pons M. 2006. New Roles for Key Residues in Helices H1 and H2 of the *Escherichia coli* H-NS N-terminal Domain: H-NS Dimer Stabilization and Hha Binding. J Mol Biol 359:679–689.

46. Madrid C, García J, Pons M, Juárez A. 2007. Molecular evolution of the H-NS protein: Interaction with Hha-like proteins is restricted to *Enterobacteriaceae*. J Bacteriol 189:265–268.

47. Hołówka J, Zakrzewska-Czerwińska J. 2020. Nucleoid Associated Proteins: The Small Organizers That Help to Cope With Stress. Front Microbiol 11:1–7.

48. Rakibova Y, Dunham DT, Seed KD, Freddolino L. 2024. Nucleoid-associated proteins shape the global protein occupancy and transcriptional landscape of a clinical isolate of *Vibrio cholerae*. J Bacteriol.

49. Ge P, Rashid FZM, Dame RT. 2025. The role of nucleoid-associated proteins in mediating responses to environmental changes. Curr Opin Microbiol 87:102628.

50. Prieto AI, Kahramanoglou C, Ali RM, Fraser GM, Seshasayee ASN, Luscombe NM. 2012. Genomic analysis of DNA binding and gene regulation by homologous nucleoid-associated proteins IHF and HU in *Escherichia coli* K12. Nucleic Acids Res 40:3524–3537.

ACKNOWLEDGMENTS

I am sincerely grateful to Prof. Tetsuya Iida for providing me with the opportunity to undertake my doctoral research in his laboratory. Working on *Vibrio parahaemolyticus*, a pathogen of long-standing scientific importance, has been both a challenging and rewarding experience. I appreciate his support and encouragement throughout my PhD training.

My deepest gratitude goes to Dr. Shigeaki Matsuda, whose mentorship, guidance, and unwavering support were central to my doctoral training. His dedication to research on pathogenic bacteria, along with his scientific rigor and integrity, profoundly shaped my development both as a researcher and as an individual. Working closely under his supervision inspired me to continuously improve and to grow into a more responsible and independent scientist.

I sincerely thank Dr. Eiji Ishii for his guidance and for the many insightful discussions that encouraged critical thinking and deeper consideration of scientific questions. I also extend my heartfelt appreciation to Dr. Andre Pratama, who was always willing to listen and engage in thoughtful discussions whenever I encountered difficulties in my research. His patience, openness, and encouragement were instrumental in fostering my independence and confidence as a researcher.

I would like to acknowledge the former members of the Iida laboratory (Dr. Pranee Somboonthum, Dr. Delly Chipta Lestari, and Dr. Dhira Saraswati Anggramukti) and the current members (Annisa Aulia Maghfirani Sudarmadi, Wethaka Loktumraks, and Ayami Morita) as well as Dr. Mohamad Imad Al Kadi and Asmaa Alzoubi. I am grateful for the

stimulating discussions and the shared experiences that made this PhD journey over the past four years both meaningful and memorable.

I also appreciate the kind assistance provided by Mrs. Natsuko Konishi-Attwood of the Iida Laboratory and Mrs. Utako Onoyama from the Office for Research Promotion (RIMD), particularly for their support with administrative procedures despite my limited proficiency in the Japanese language.

My deepest gratitude goes to my family and friends for their constant encouragement, especially during challenging times. I am thankful to my father, Tan Totok Wibowo, whose humor helped lift my spirits; to my mother, Ie Sien Lian Nio, whose prayers sustained me; and to my sister, Tan Oktaviany Wibowo, who was always willing to listen and offer support.

Finally, I sincerely thank the BIKEN Foundation for supporting my doctoral studies in Japan through the Taniguchi Scholarship Program. I hope that the knowledge and experience gained at RIMD and the Graduate School of Frontier Biosciences, The University of Osaka, will serve as a solid foundation for my future career and enable me to contribute meaningfully to society through scientific research.

AUTHOR'S ACHIEVEMENT

Publication

Tan Paramita Wibowo Sutanto, Andre Pratama, Eiji Ishii, Tetsuya Iida, Shigeaki Matsuda. TsrA modulates type III secretion system 2 expression as a co-regulator of H-NS in *Vibrio parahaemolyticus*. (The manuscript is already submitted and currently under review)

Conference

1. **Tan Paramita Wibowo Sutanto**, Andre Pratama, Eiji Ishii, Tetsuya Iida, Shigeaki Matsuda. TsrA-Mediated Gene Regulation in *Vibrio parahaemolyticus*. FY2024 Research Achievement Presentation of Research Institute for Microbial Diseases. 24 January 2025. Poster presentation.
2. **Tan Paramita Wibowo Sutanto**, Andre Pratama, Eiji Ishii, Tetsuya Iida, Shigeaki Matsuda. TsrA-Mediated Gene Regulation in *Vibrio parahaemolyticus*. The 98th Annual Meeting of Japanese Society of Bacteriology. 29-31 May 2025. Poster presentation.
3. **Tan Paramita Wibowo Sutanto**, Andre Pratama, Eiji Ishii, Tetsuya Iida, Shigeaki Matsuda. TsrA-Mediated Gene Regulation in *Vibrio parahaemolyticus*. The 57th Vibrio Symposium. 30-31 October 2025. Oral presentation.
4. **Tan Paramita Wibowo Sutanto**, Andre Pratama, Eiji Ishii, Tetsuya Iida, Shigeaki Matsuda. TsrA-Mediated Gene Regulation in *Vibrio parahaemolyticus*. The 78th Kansai Branch Meeting of the Japanese Society for Bacteriology. 3 November 2025. Oral presentation.

5. **Tan Paramita Wibowo Sutanto**, Andre Pratama, Eiji Ishii, Tetsuya Iida, Shigeaki Matsuda. TsrA modulates type III secretion system 2 expression as a co-regulator of H-NS in *Vibrio Parahaemolyticus*. FY2025 Research Achievement Presentation of Research Institute for Microbial Diseases. 23 January 2026. Oral presentation.

Awards

1. Best Poster Award. FY2024 Research Achievement Presentation of Research Institute for Microbial Diseases. 24 January 2025. Poster presentation.
2. Student Excellence Presentation Award. The 78th Annual Meeting of the Kansai Branch of the Japanese Society for Bacteriology. 3 November 2025. Oral presentation.